ELECTRONIC MATERIALS AND APPLICATIONS (EMA 2022)

Simulation-based resonant imaging of electronic materials for enhanced design in 5G and other emerging technologies

Marzena Olszewska–Placha*, Malgorzata Celuch, Janusz Rudnicki

QWED Sp. z o.o., Warsaw, Poland

S12: 5G Materials and Applications Telecommunications

Outline

- ❑ Electromagnetic modelling & simulations – development & applications by QWED.
- ❑ Modelling-based resonant material characterisation techniques for 5G and other emerging technologies.
- ❑ Advances in resonator-based characterisation techniques - 2D imaging of material parameters.
- ❑ Broadband mm-wave characterisation of materials.
- ❑ Conclusions & outlook.

Polish high-tech SME - 25 years on the world's market

Business branches and competences

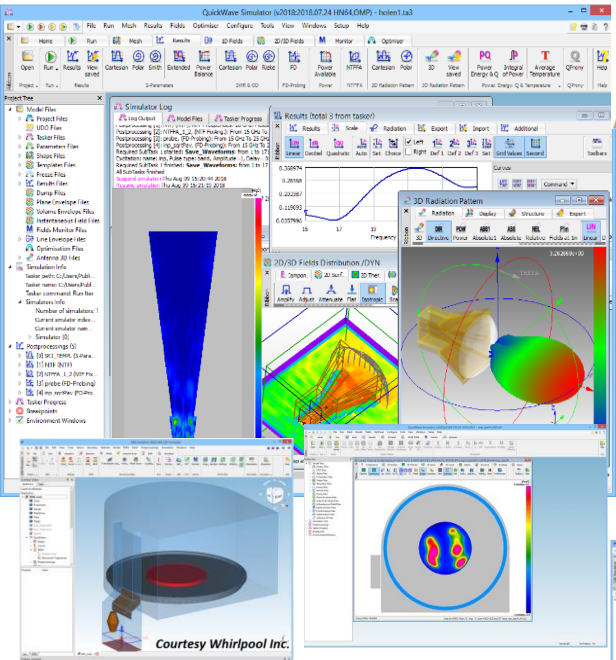

Electromagnetic and Multiphysics simulation & design software QuickWave

based on 300+ publications by the founders

Consultancy & design services based on EM expertise & tools

team of 10+engineers, 4 PhDs, 2 Profs

key areas: *MW power appliances, customised resonators, antennas &feeds*

Microwave applicator for bituminous surfaces and dual-reflector antenna designed by QWED team with QuickWave software

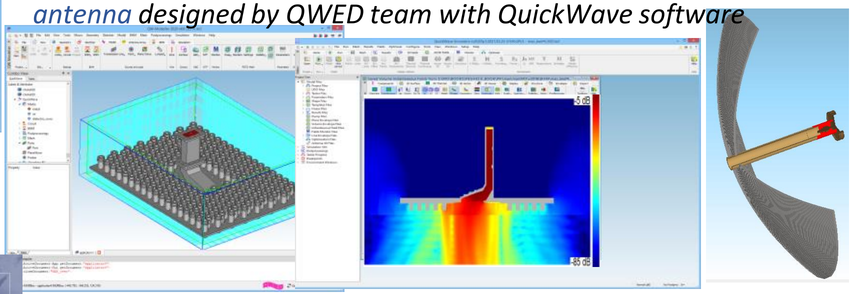

Courtesy Whirlpool Inc.

Test-fixtures for precise material measurements

based on 300+ publications by prof.J.Krupka, IEEE Fellow

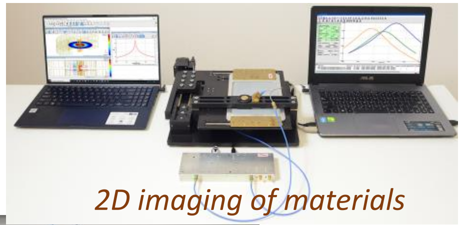

2D imaging of materials

Characterisation of battery materials

Millimetre-wave characterisation of materials for 5G

R&D projects

FP6 SOCOT – development and validation of an optimal methodology for overlay control in semiconductor industry, for the 32 nm technology node and beyond.

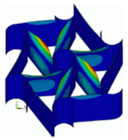

FP6 CHISMACOMB – development, modelling, and applications of chiral materials → EM validation of mixing rules

Eureka E! 2602 MICRODEFROST MODEL – innovative software-based product development tool for simulating and optimising heating and defrosting processes in microwave ovens

FP7 HIRF SE (High Intensity Radiated Field Synthetic Environment) - numerical modelling framework for aeronautic industry

Eureka FOODWASTE – developing new microwave treatment system for high water content waste

ERA-NET MNT NACOPAN – applications and modelling of nano-conductive polymer composites

NGAM2 – designing an industrial device for thermal bonding of bituminous surfaces with the aid of microwave heating

MMAMA (Microwave Microscopy for Advanced and Efficient Materials Analysis and Production) – accelerating the development of high efficiency solar cells through application and enhancement of material measurement techniques

NanoBat - developing a novel nanotechnology toolbox for quality testing of Li-ion and beyond Lithium batteries with the potential to redefine battery production in Europe and worldwide.

ULTCC6G_EPac - developing a novel functional materials and their processing techniques feasible for 5G and beyond.

Modelling – based characterisation of materials for emerging technologies

Focus on dielectric resonators:

- ❑ proven ultra-high acccuracy in GHz range (0.3% for Dk, IEC 61189-2-721:2015)
- ❑ dedicated to low-loss & low-resitivity materials (both, bulk and thin sheets)
- ❑ ease-of-use
- ❑ available on the market
- ❑ Point-wise technique extendable to surface mapping operation regime
- ❑ repeatability & reproducibility for 5G under independent studies (iNEMI project)

Resonator methods – motivation and background (1)

Resonance in practice: given fixed strength of Signal(in), at resonance Signal (out) is strongest

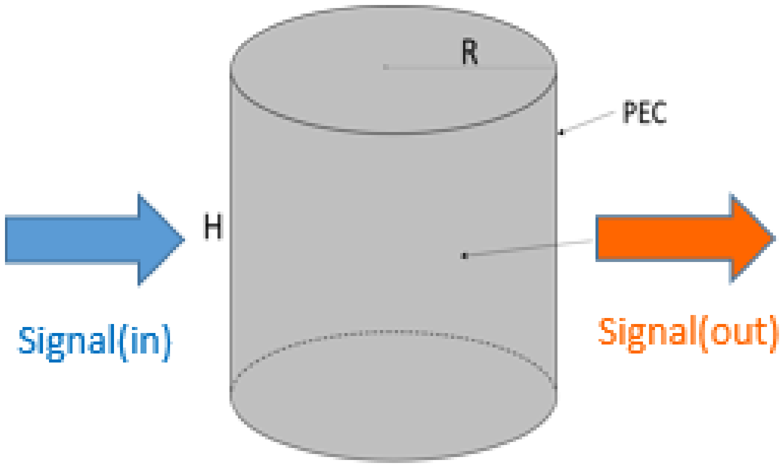

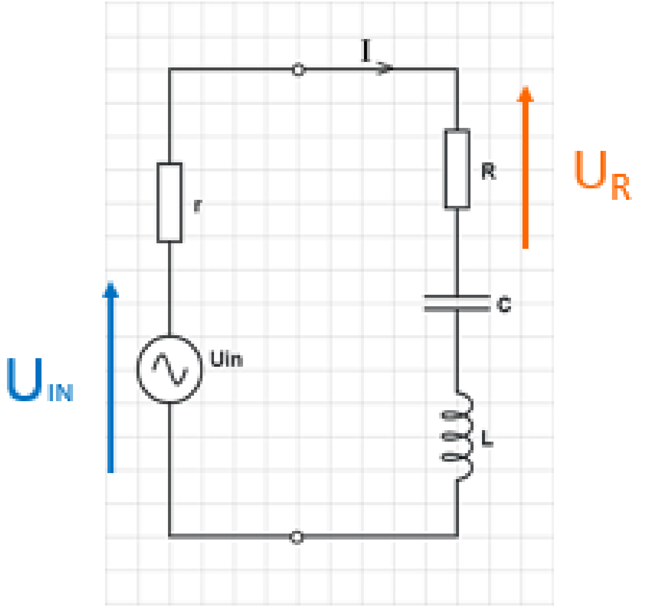

δ(t)

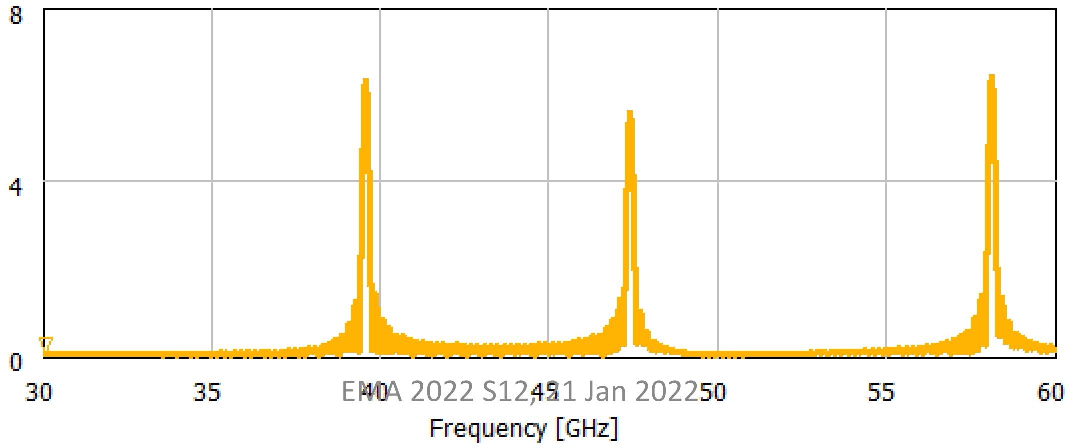

Resonator methods – motivation and background (2)

Resonance in theory: **non-zero electromagnetic fields exist in isolated structures (no excitation).**
Field properties are well-defined and linked to material properties.
E.g. for cylindrical cavities:

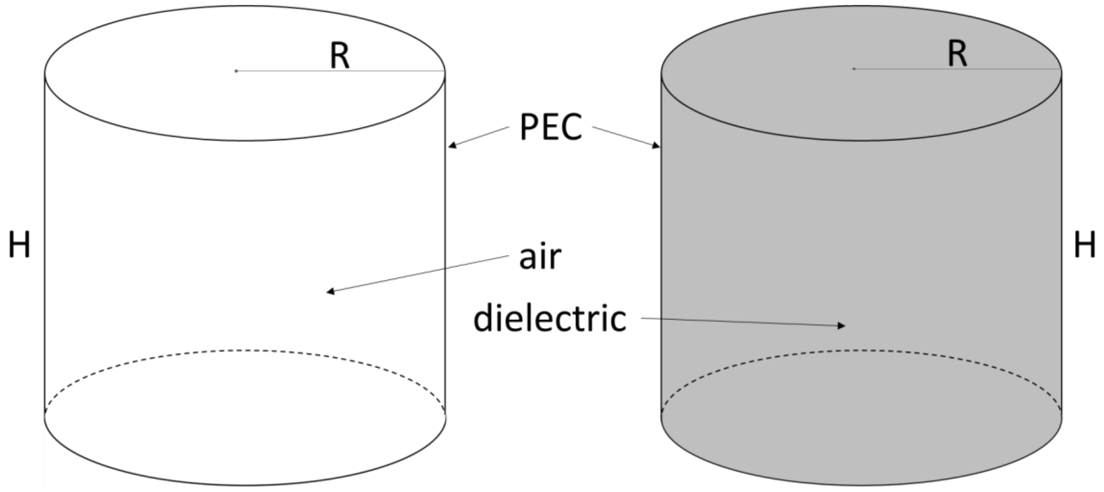

$$f_{r,mnp} = \frac{c}{\sqrt{Dk}} \sqrt{\left(\frac{\kappa_{mn}^{(,)}}{\pi R}\right)^2 + \left(\frac{p}{H}\right)^2}$$

in non-magnetic low-loss dielectrics

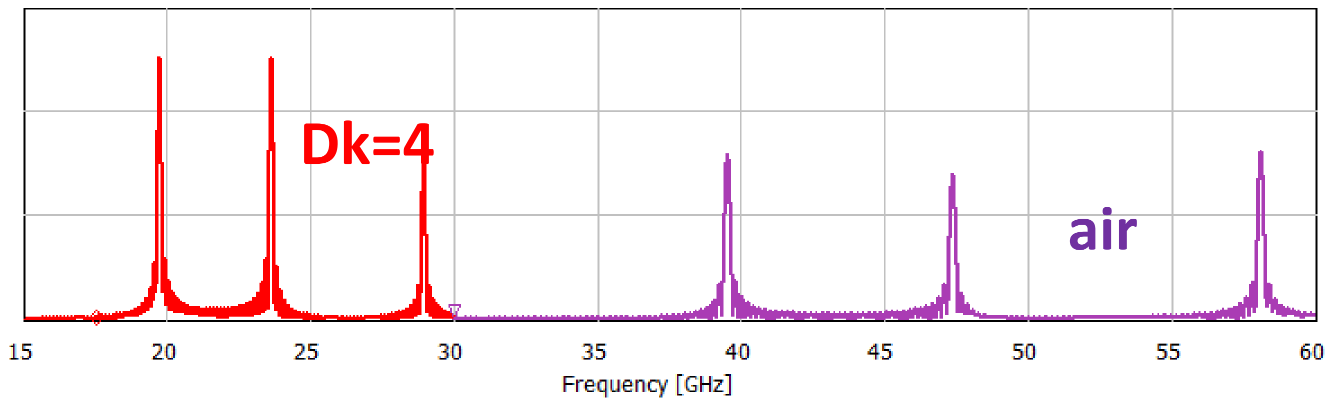

$$Q = 2\pi \frac{\iiint_V \varepsilon \vec{E} \cdot \vec{E}^* dv}{T \iiint_V \sigma \vec{E} \cdot \vec{E}^* dv} = \frac{\omega\varepsilon}{\sigma} = \frac{1}{Df} \approx \frac{fres}{\Delta f}$$

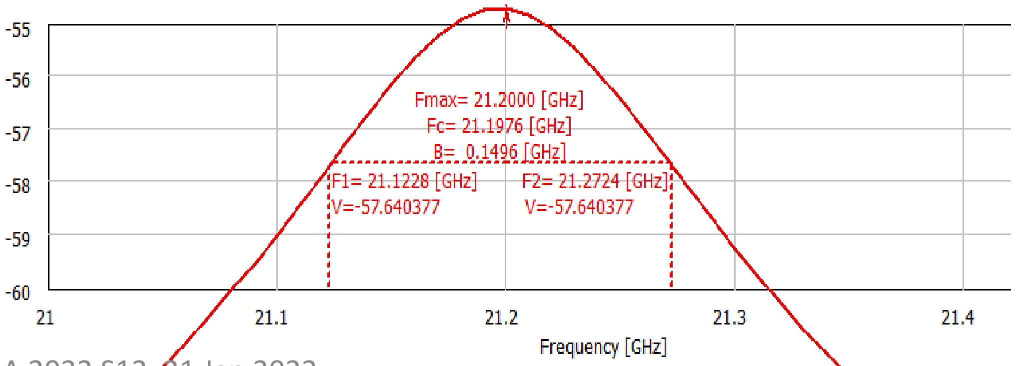

Analytical solutions are for eigenvalue problems.
Measurement problems are deterministic (cavity is coupled to source & load).

Cylindrical resonator: single-mode versus multi-mode operation

TE011 mode

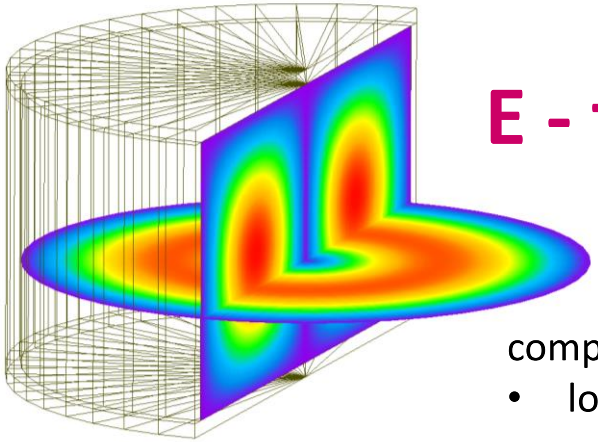

E - field

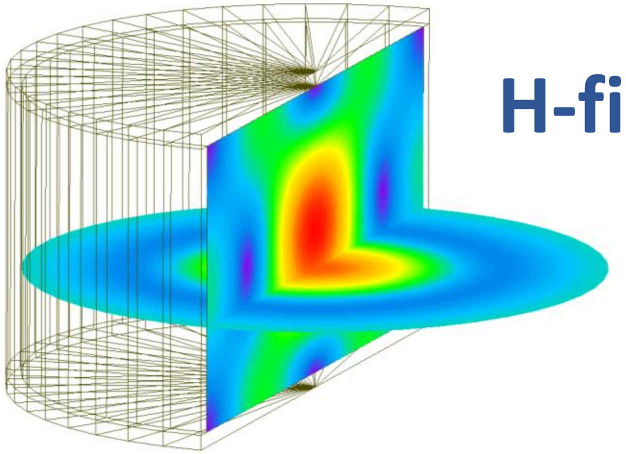

H-field

compared to rectangular (cuboidal) cavities, typically:

- lower contribution of wall losses
- easier standard manufacturing

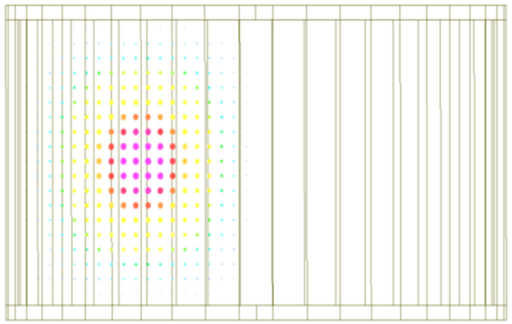

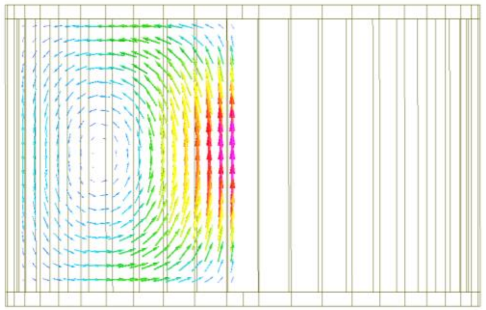

TE021 mode

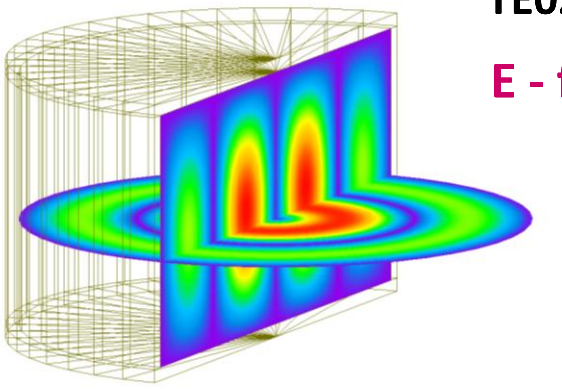

E - field

- ❑ Resonators are multimode devices hence formally, material measurement can be performed at many frequencies in the same resonator.
- ❑ Some modes provide highest accuracy of material characterization. Some are difficult to excite.
- ❑ Software provided with the resonator in compatible only with modes pre-selected by the vendor.
- ❑ Single mode resonators: SPDR, SiPDR, SCR
- ❑ Multi-mode resonators: BCDR and FPOR.

Split-Post Dielectric Resonator (SPDR) - basics

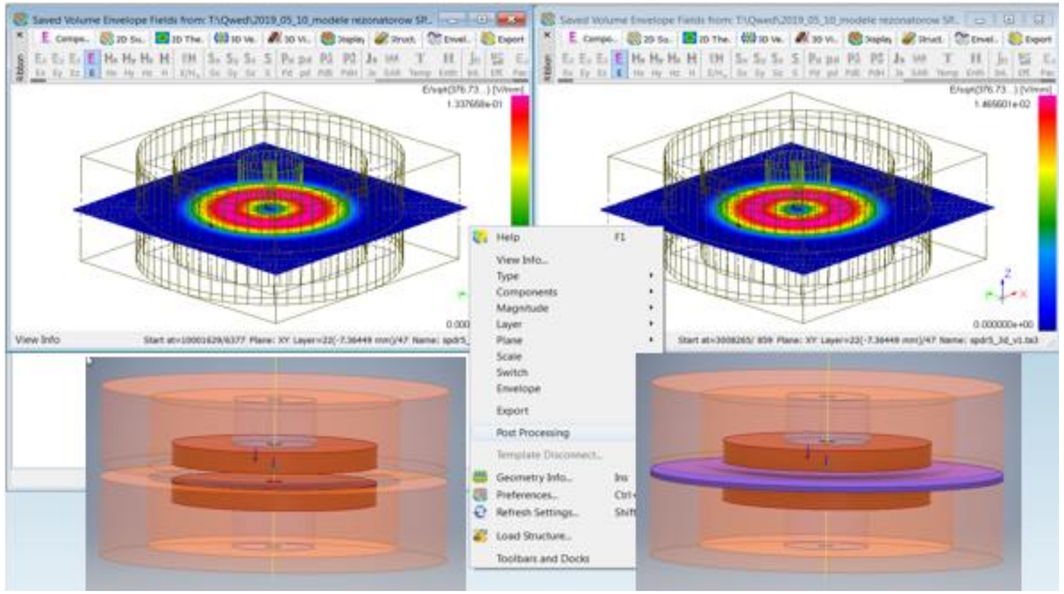

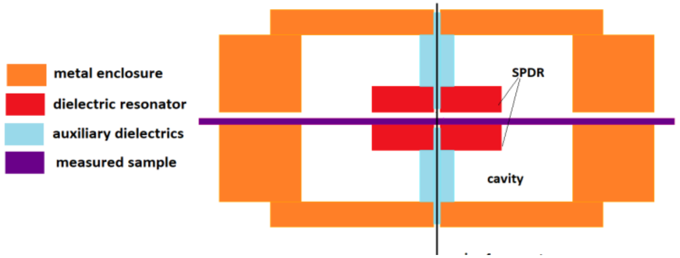

For laminar dielectrics and high-resistivity semiconductors

- resonant mode with EM fields mostly confined in and between those ceramic posts → minimial losses in metal enclosure
- H-field is only vertical at the side wall of the enclosure → circumferential currents → no radiation through slot
- E-field tangential to SUT → air slots between SUT and posts have negligible effect
- **easy SUT insertion through slot, no dismantling**
- Field patterns remain practically unchanged but resonant frequencies and Q-factors change, providing information about SUT material parameters

SUT of $\varepsilon_s = \varepsilon_s' - j\,\varepsilon_s''$ is inserted into DR:
resonant frequency changes from f_e to f_s
Q-factor changes from Q_e to Q_s.

$$\frac{f_e - f_s}{f_e} \approx \frac{h}{2C}\iint_S \left[\varepsilon_s'(x,y) - 1\right]\left|E(x,y)\right|^2 dS$$

$$\frac{1}{Q_s} - \frac{1}{Q_e} \approx \frac{h}{C}\iint_S \varepsilon_s''(x,y)\,E^2(x,y)\,dS$$

$$C = \iiint_V \left|E(x,y)\right|^2 dV$$

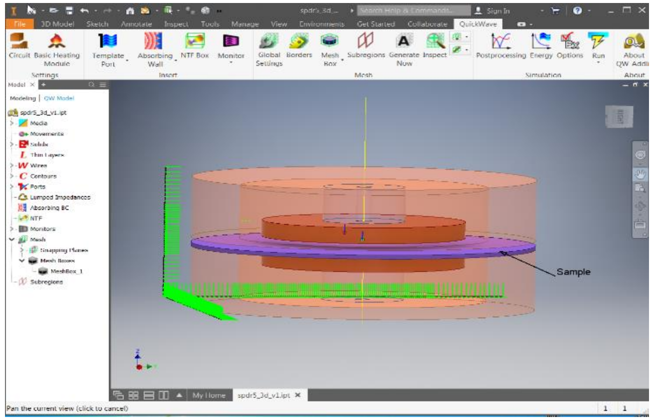

Full 3D model of 10GHz SPDR in QW-AddIn for Autodesk® Inventor® Software
(common environment for modelling & manufacturing)

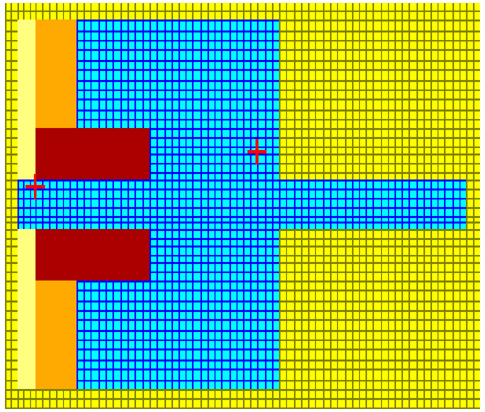

Axisymmetrical 2D BOR model full EM information
economies in computer effort : 10^3 or more

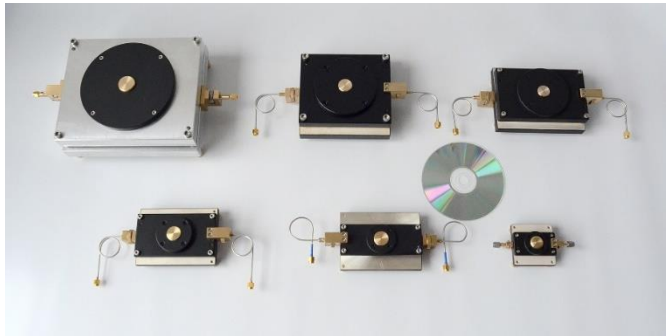

Split-Post Dielectric Resonator (SPDR) – modelling results

Sample in strong E-field nearly constant between the two posts

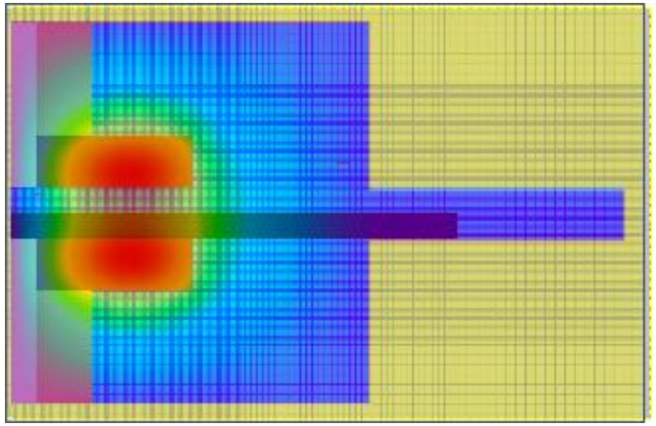

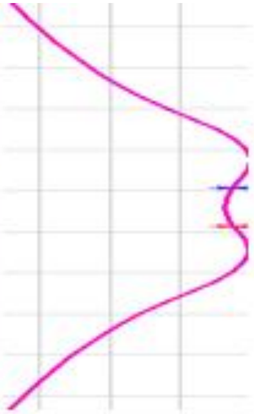

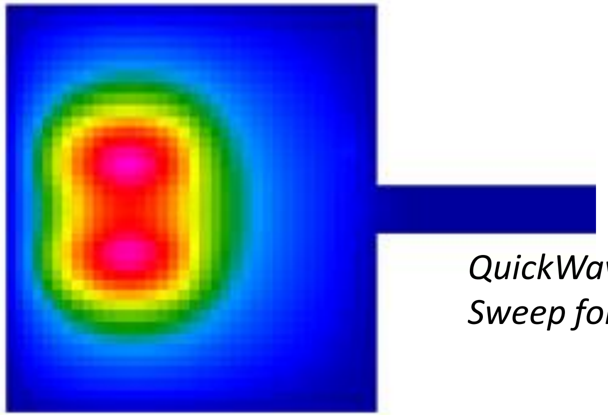

QuickWave simulations of 2.5GHz SPDR performed in automatic Parameter Sweep for varying sample thickness (colours) and dielectric constant (eps)

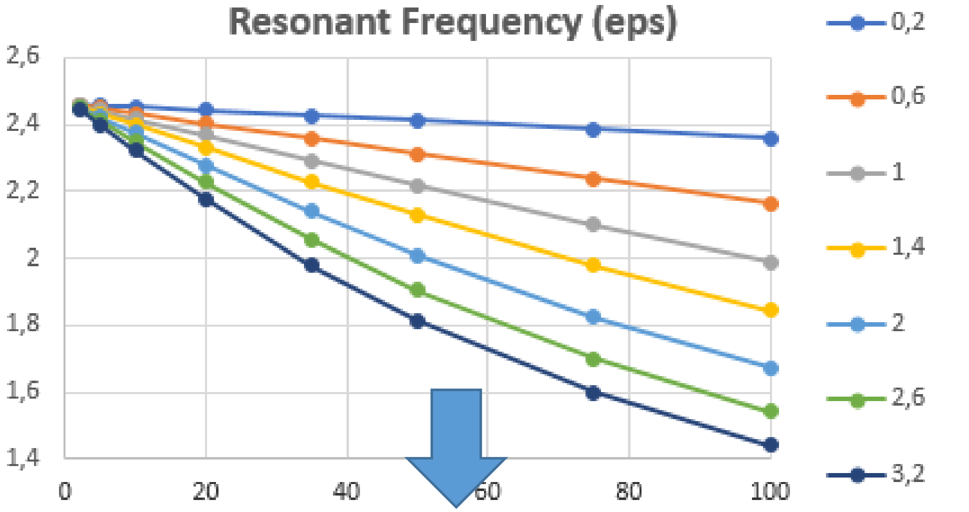

Data for dedicated software for material parameters extraction

Electric field

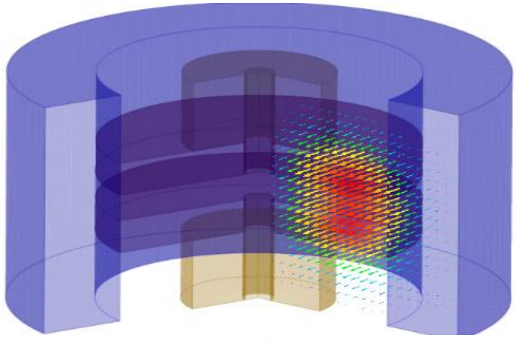

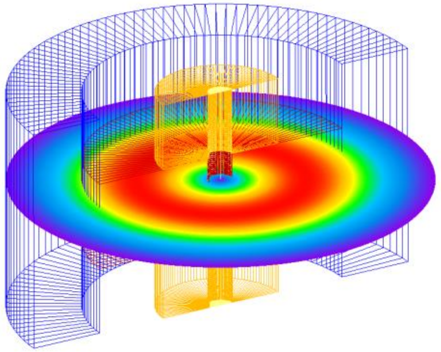

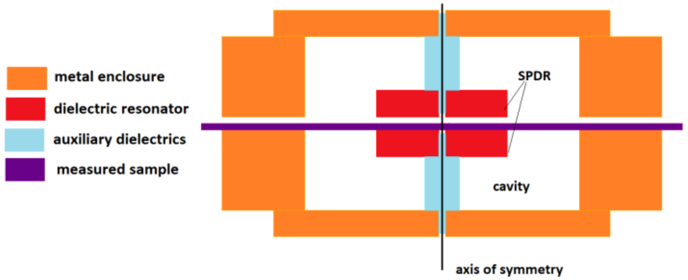

Magnetic field

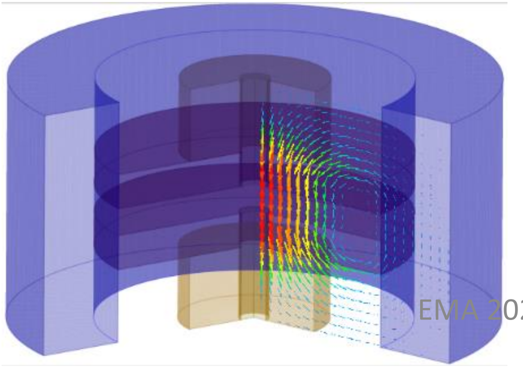

Split-Post Dielectric Resonator (SPDR) – operation (1)

Operation workflow – with the use of Q-Meter

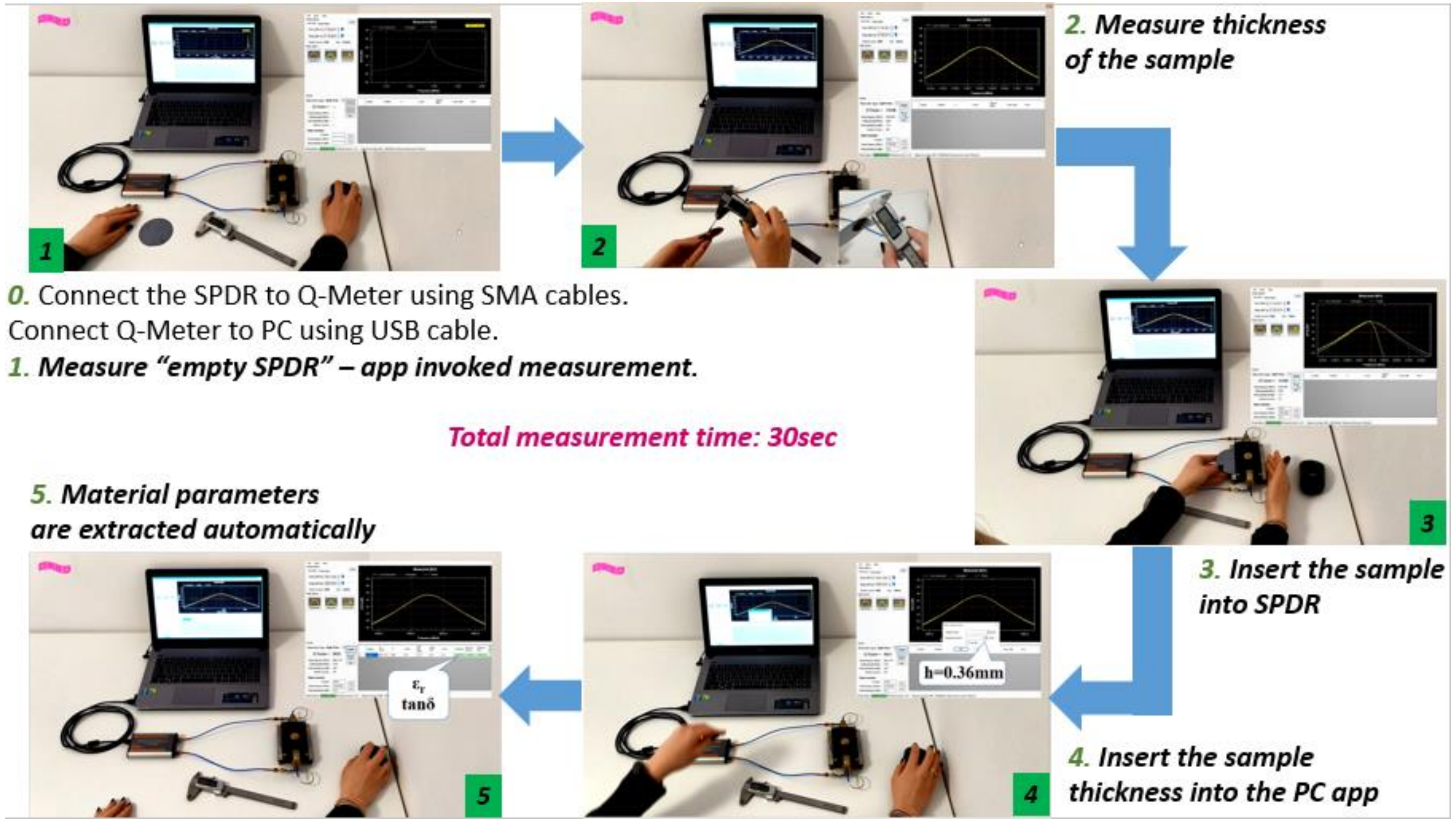

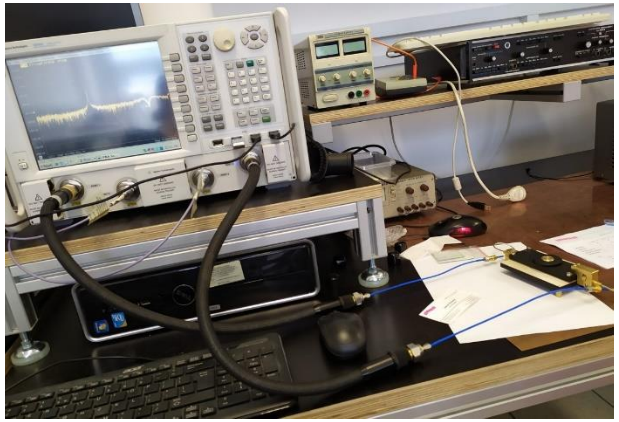

SPDR use in labs...

...and at home

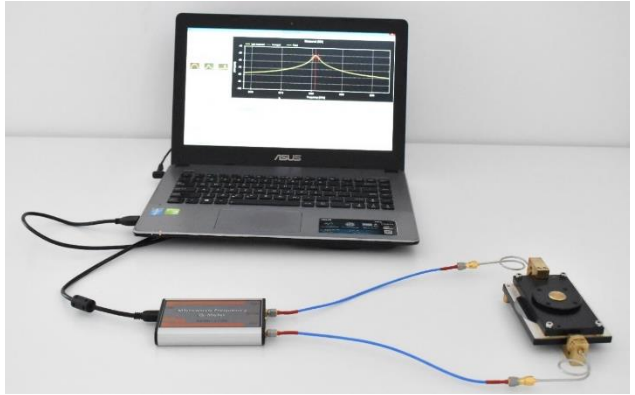

For many practical materials, measuring only abs (S21) provides appropriate accuracy.

Keysight Option N1500A uses S21 (amplitude & phase) which helps enhance accuracy (*under study in iNEMI project*).

Antenna & feed systems design – for various applications

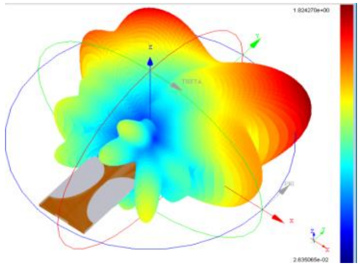

Balanced antipodal Vivaldi antenna & 3D radiation pattern at 10 GHz.

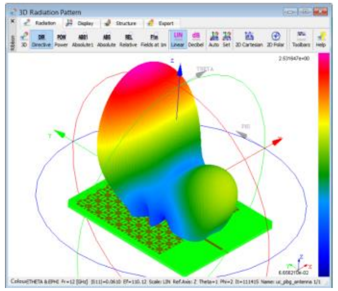

Aperture-coupled patch antenna on uniplanar photonic bandgap substrate & its radiation pattern at 12 GHz.

Antenna arrays for 5G and automotive radar application

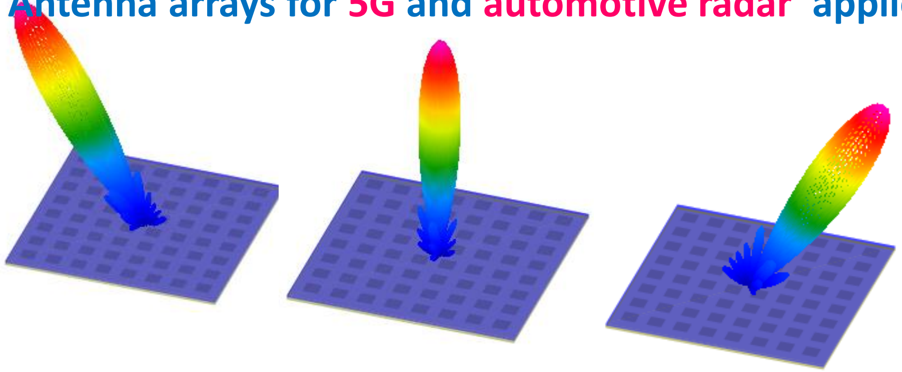

Designing and verifying tracking capabilities

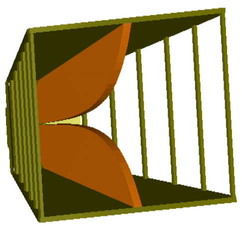

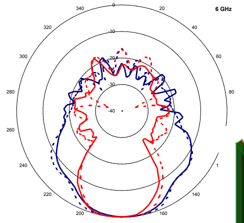

Pyramidal horn antenna for military surveillance measured (courtesy prof.B.Stec) & simulated patterns

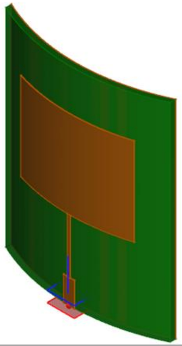

Planar antennas for smart bio-sensors

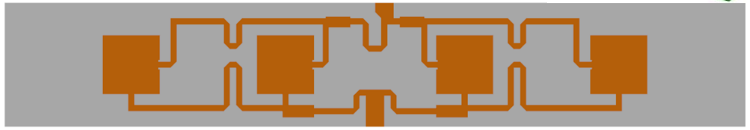

Antenna feed systems designed by NRAO

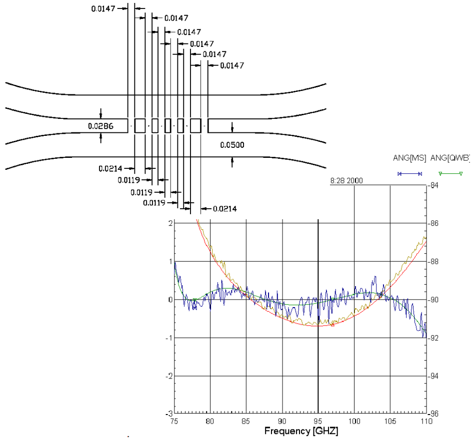

QuickWave 3D results at NRAO, see: ALMA Memos 381, 343, 325, 278.

Large dual reflector antennas: *Cassegrain, Gregorian, etc.*

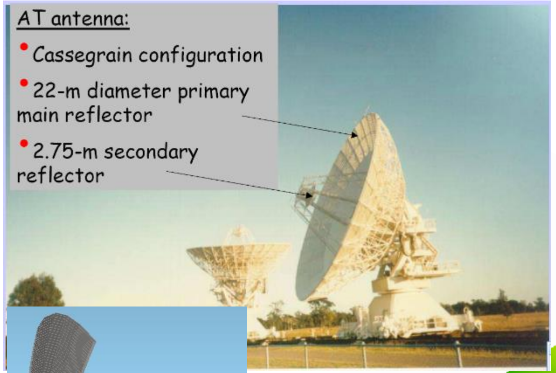

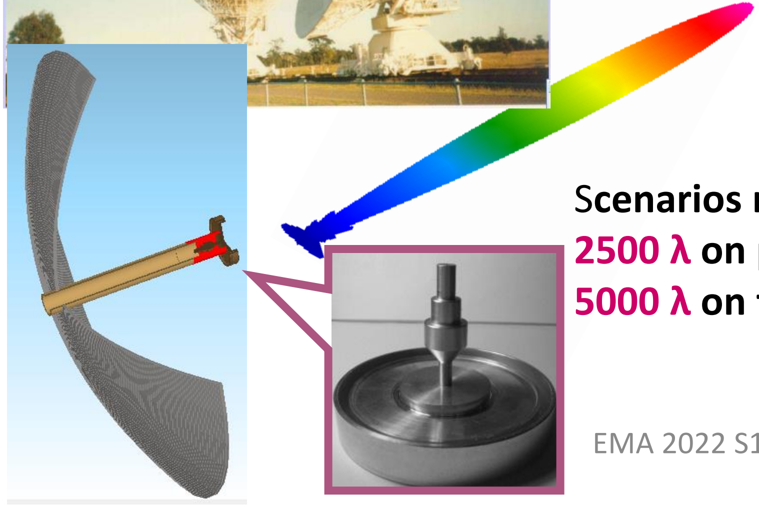

BOR FDTD

Unique, ultra-fast vector 2D Bessel & FDTD hybrid solver for design & analysis of devices with axial symmetry

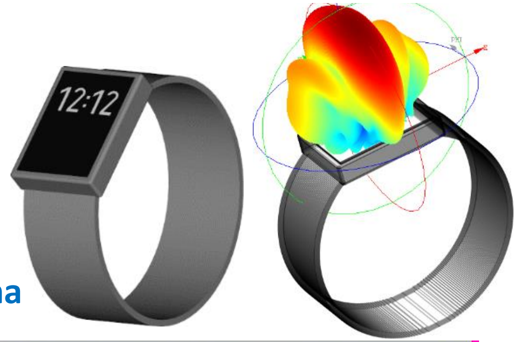

Smartwatch with embedded patch antenna

Scenarios modelled full-wave:
2500 λ on popular PC
5000 λ on top-shelf PC

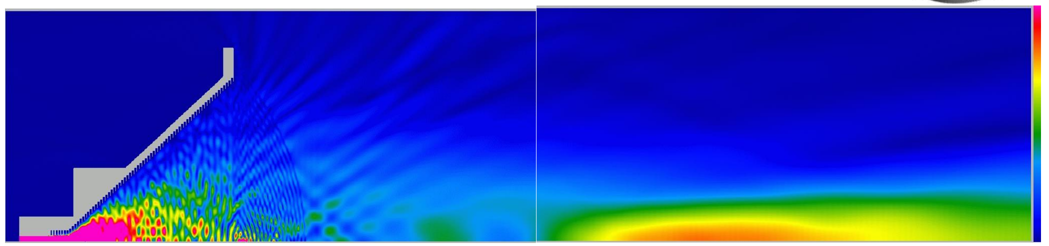

Corrugated horn antenna for material measurements

Dedicated simulation & display regimes for 5G patch antenna analysis

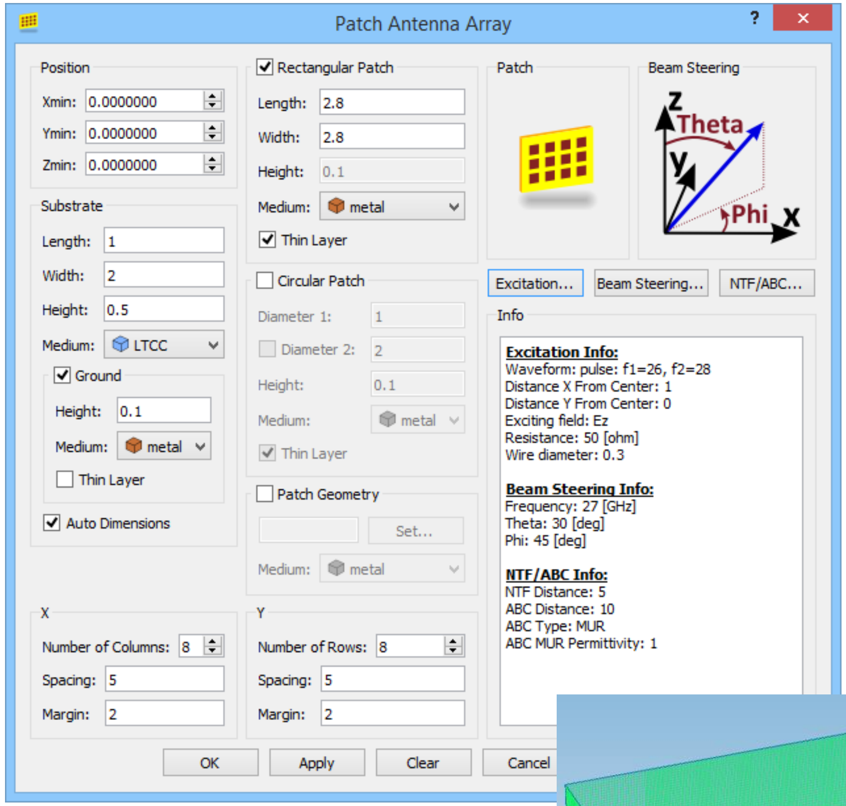

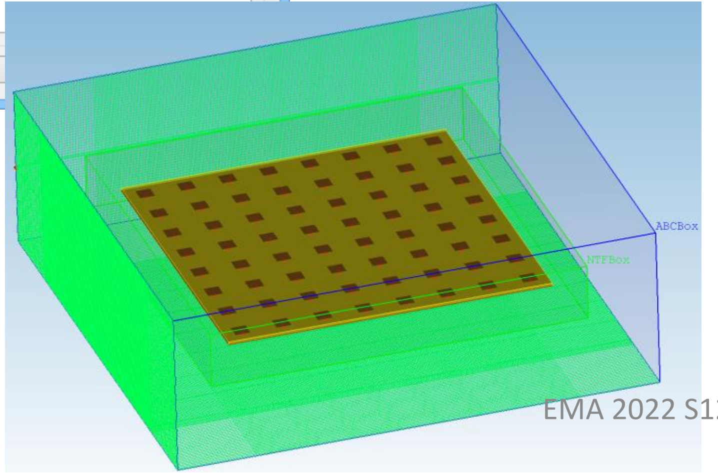

LTCC-based 8x8 patch array

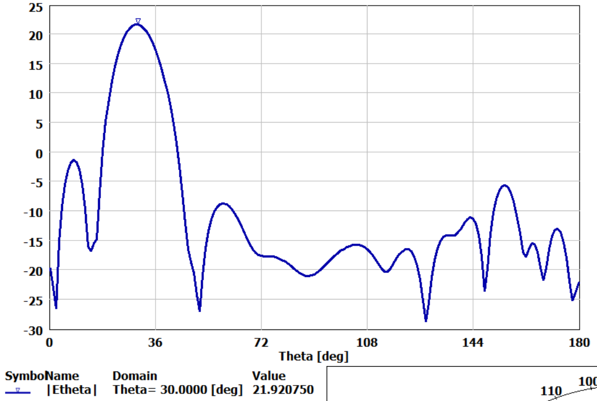

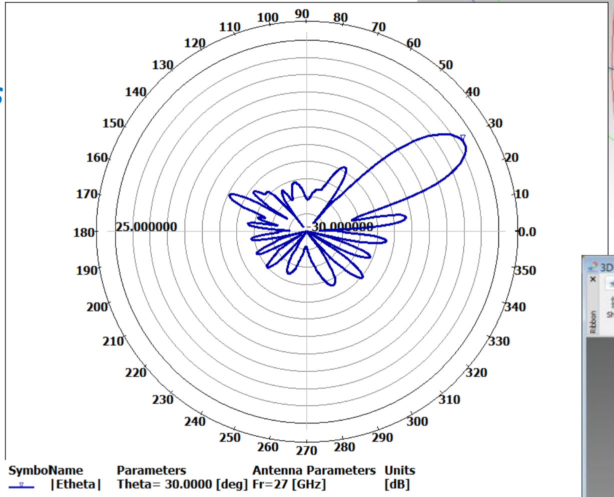

2D radiation patterns

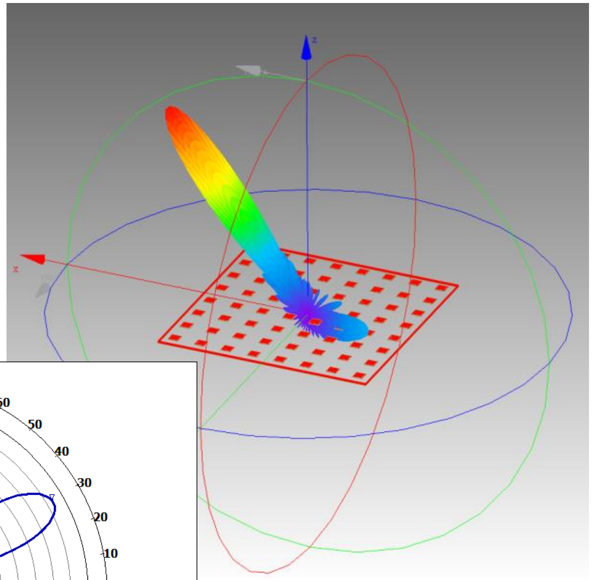

3D radiation pattern

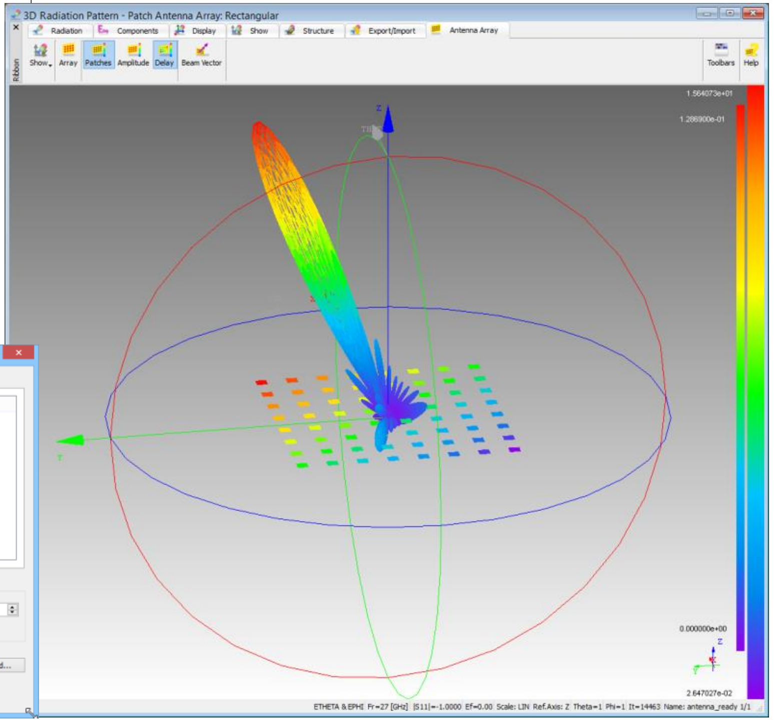

Distribution of source phase shifts across the array

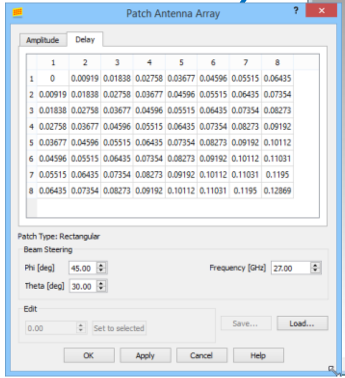

	1	2	3	4	5	6	7	8
1	0	0.00919	0.01838	0.02758	0.03677	0.04596	0.05515	0.06435
2	0.00919	0.01838	0.02758	0.03677	0.04596	0.05515	0.06435	0.07354
3	0.01838	0.02758	0.03677	0.04596	0.05515	0.06435	0.07354	0.08273
4	0.02758	0.03677	0.04596	0.05515	0.06435	0.07354	0.08273	0.09192
5	0.03677	0.04596	0.05515	0.06435	0.07354	0.08273	0.09192	0.10112
6	0.04596	0.05515	0.06435	0.07354	0.08273	0.09192	0.10112	0.11031
7	0.05515	0.06435	0.07354	0.08273	0.09192	0.10112	0.11031	0.1195
8	0.06435	0.07354	0.08273	0.09192	0.10112	0.11031	0.1195	0.12869

Single-Post Dielectric Resonator (SiPDR) – basics

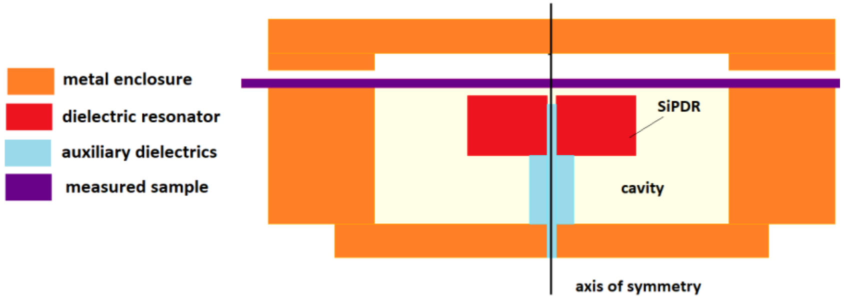

For low-resistivity semiconductors and conducting thin films

sample between the **single post dielectric** and the **ground plane**

weak E-field in sample plane
note: tangential E-field is zero at ground plane;
it increases linearly in –z direction towards sample plane

measurement of very lossy samples possible
but measurement sensitive to sample position in z-direction

measures **resistivity or sheet resistance**

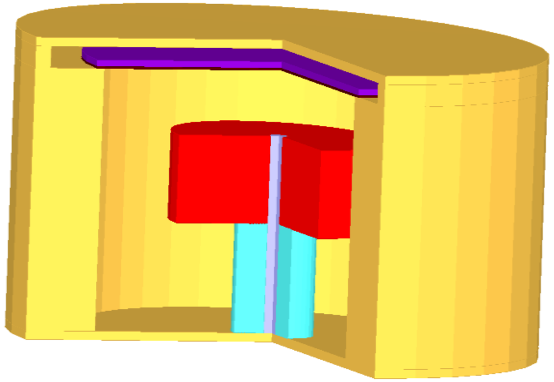

Simulation model in QuickWave software

EM simulation results obtained with QuickWave software

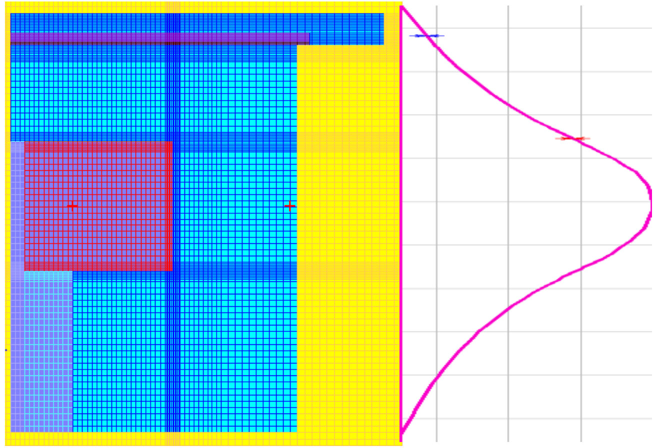

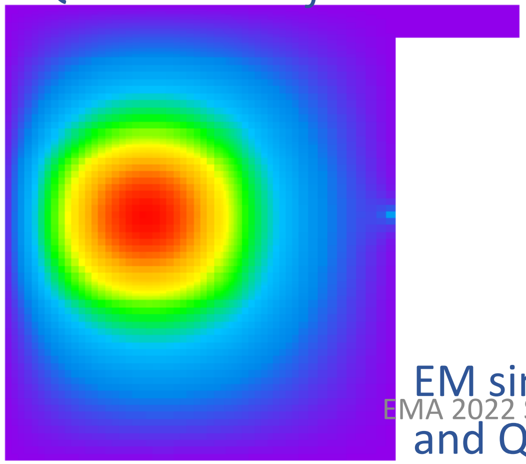

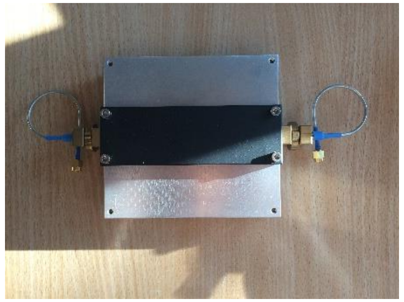

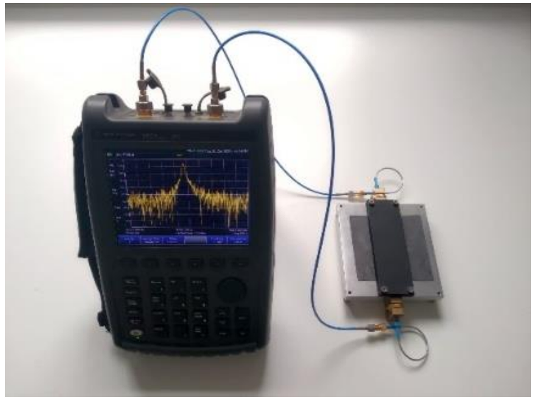

SiPDR @5GHz and its measurement setup with VNA

EM simulations analyse changes of resonant frequency and Q-factor as a function of sample's resistivity

Single-Post Dielectric Resonator (SiPDR) – measurements

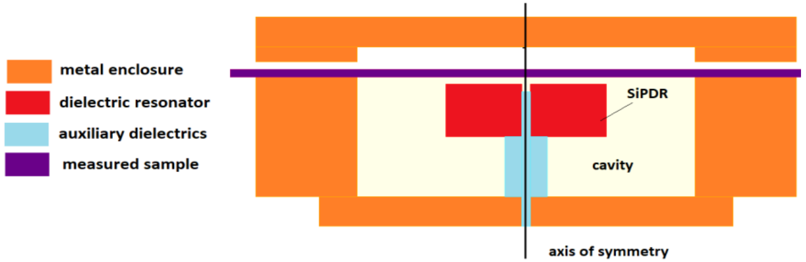

SiPDR applies for:

- ✓ Low-resistivity semiconducting materials
- ✓ Thin resistive layers, e.g. screen-printed composite layers
- ✓ Carbon-based anodes for battery cells
- ✓ etc.

Applied for testing graphene anodes for battery cells

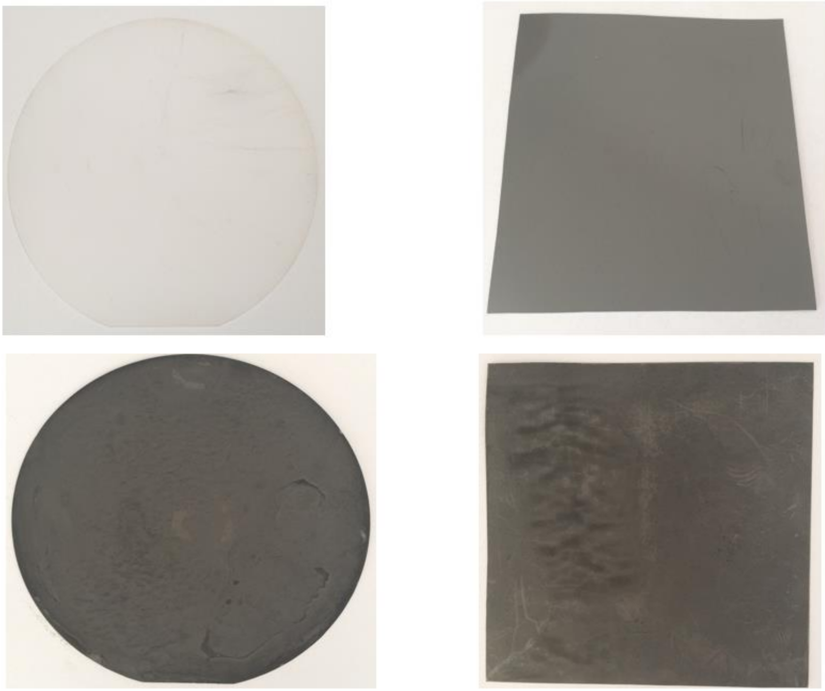

courtesy PLEIONE Energy, Greece

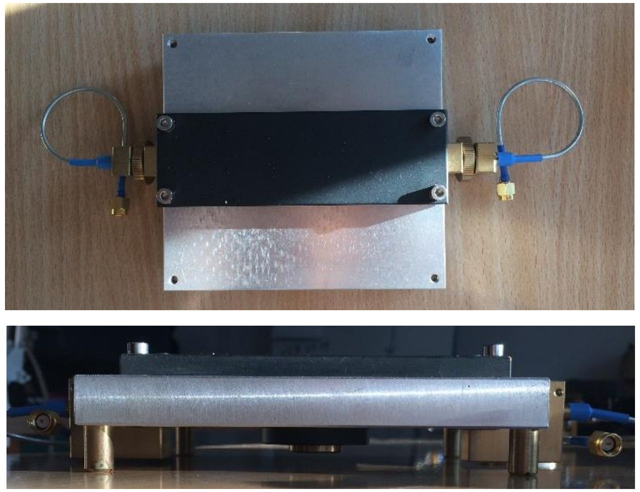

SiPDR @ 5GHz

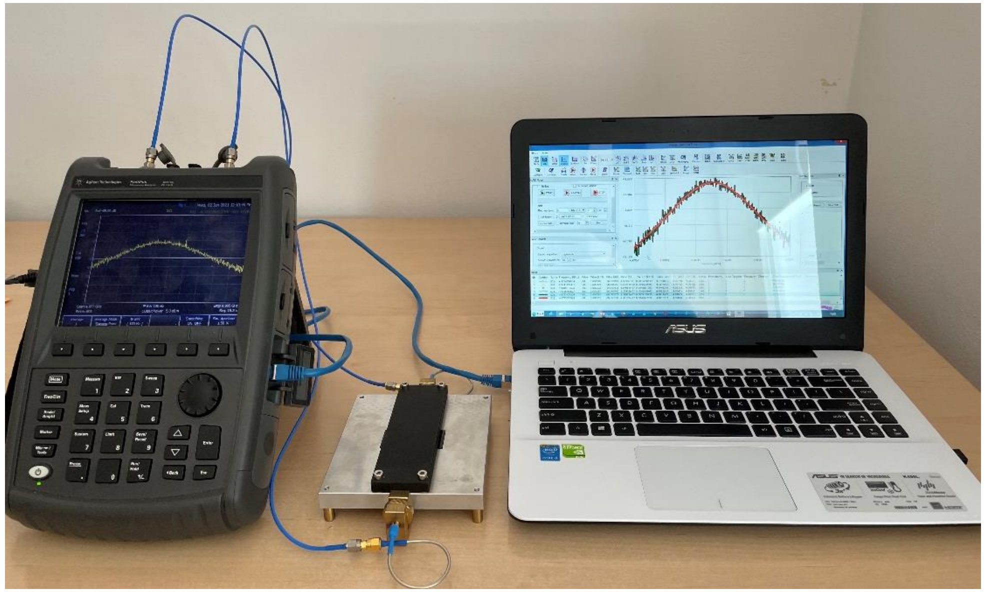

Surface resistance of GNP layers measured with SiPDR at 5GHz

Sample		Surface resistance [Ω/□]
GNP on quartz	Edge	21.485
	Centre	21.020
GNP on polymer	Edge	90.167
	Centre	25.557

2D imaging of material parameters

- 2D maps of electrical parameters: *relative permittivity* (Dk), *loss tangent* (Df), *resistivity*, or *surface resistance*
- Material homogeneity testing
- For qualitative and quantitative material testing
- Laminar dielectrics – packaging in 5G systems
- Semiconductors industry – high density packaging at a single wafer
- Battery cells materials – uniformity of electrical parameters of anodes

2D imaging of material parameters – laminar dielectrics (1)

For low-loss dielectrics and high-resistivity semiconductors

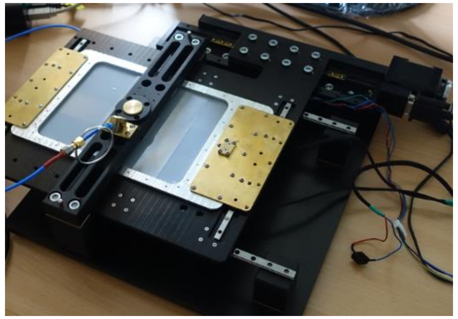

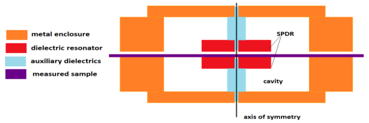

- ❑ SPDR technique based 2D scanner
- ❑ Simulation model accounting for mechanical constraints, e.g. dielectric membrane serving as sample holder
- ❑ 10GHz for higher spatial resolution

A joint product of QWED and Keysight, developed in the H2020 MMAMA project, has been acknowledged as *Innovation Radar* *of the European research.*

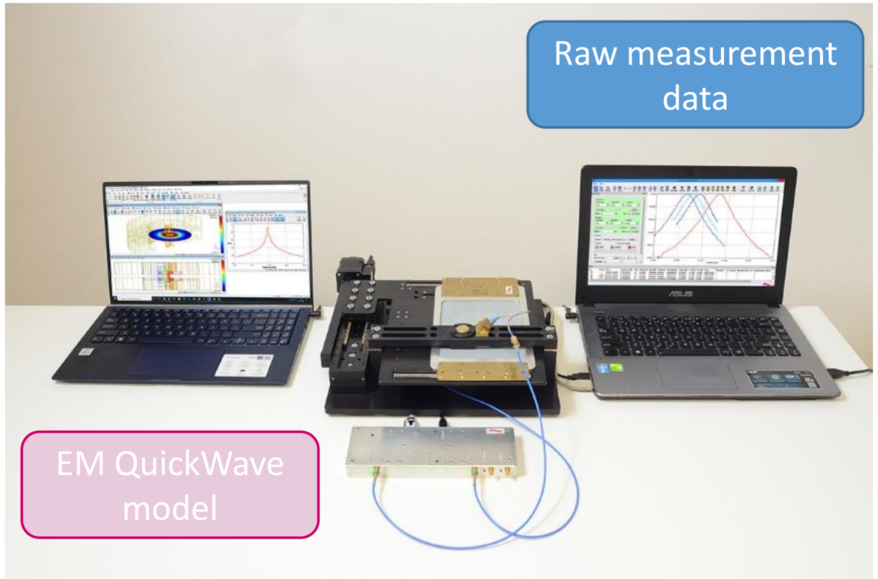

|S21| curves are for several scanning positions:

- curve max indicates resonant freq. (Dk)
- curve 3dB width indicates losses (Df)

Fully automated measurement procedure through control application

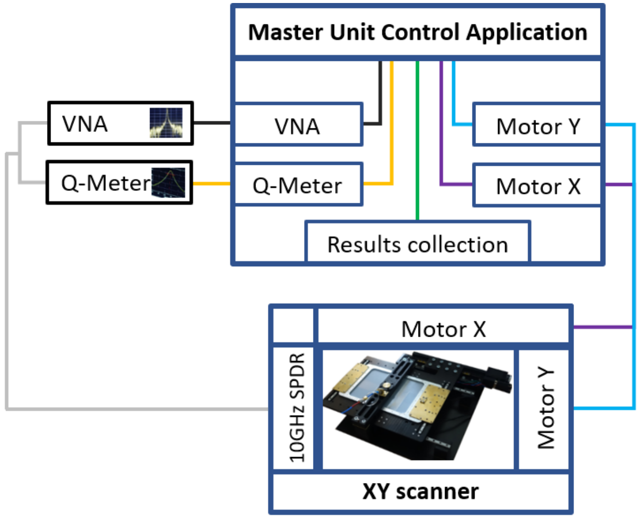

2D imaging of material parameters – laminar dielectrics (2)

For low-loss dielectrics and high-resistivity semiconductors

2D SPDR scanner @ 10GHz

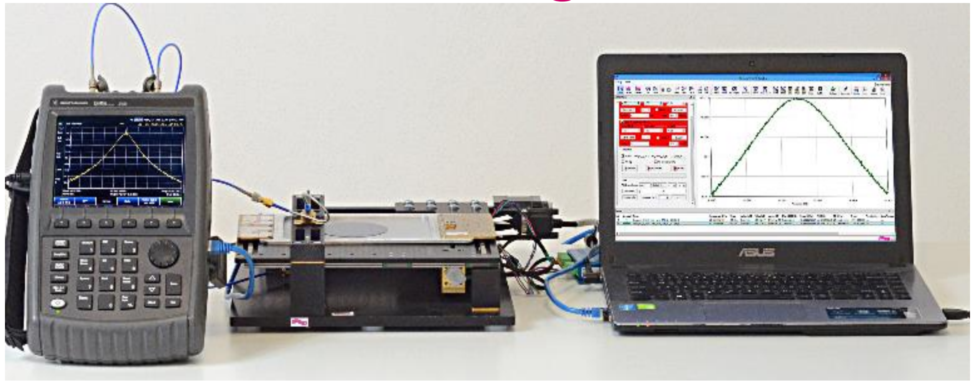

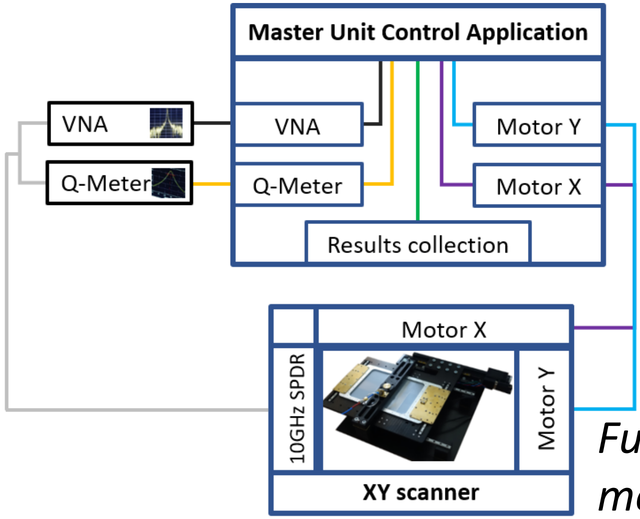

Fully automated measurement procedure

2D surface map of dielectric constant of quartz

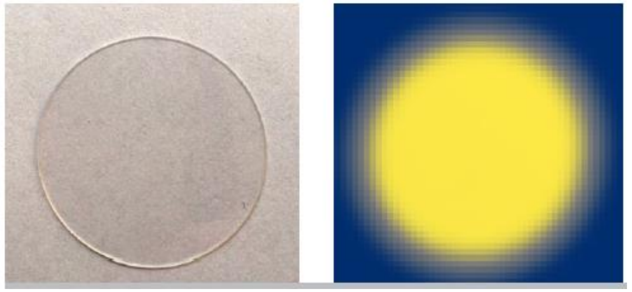

2D surface map of resistivity of semiconductor wafers

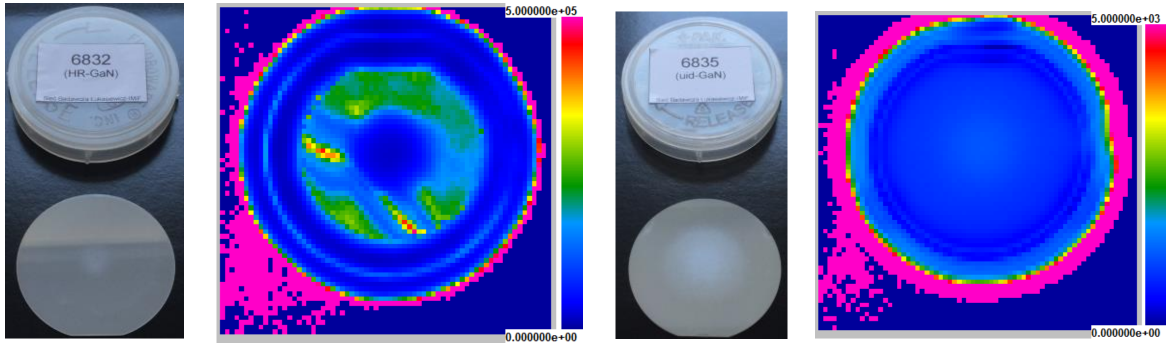

**courtesy L-IMP, Poland*

2D surface map of measured Q-factor of „QWED" pattern made of organic semiconductor deposited on quartz

Raw data image

Data post-processed using field pattern simulated in QuickWave

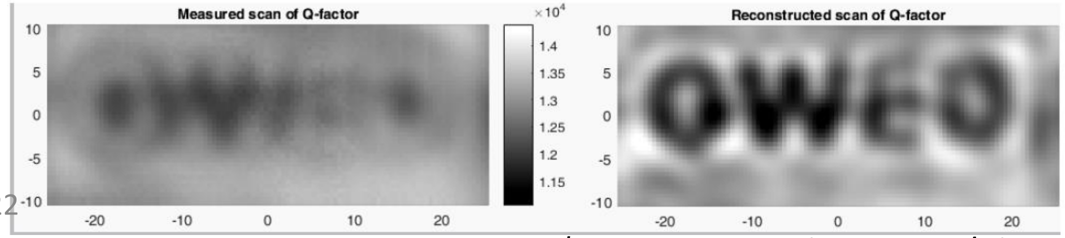

**courtesy MateriaNova, Belgium*

2D imaging of material parameters – conducting materials (1)

For semiconducting and low-resistivity materials

- SiPDR technique based 2D scanner
- Simulation model accounting for XY translation table constraints, i.e. inverter configuration required
- 10GHz for higher spatial resolution

Conceptual mechanical design of 2D surface scanner

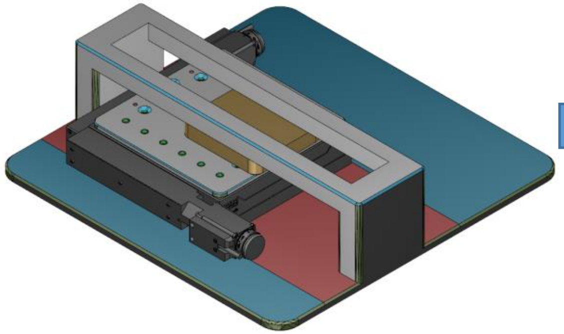

Electromagnetic design of 10GHz SiPDR

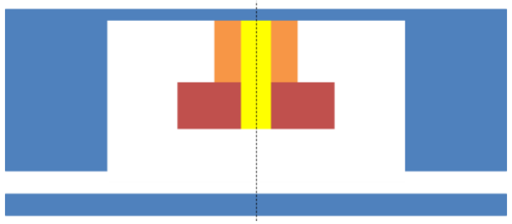

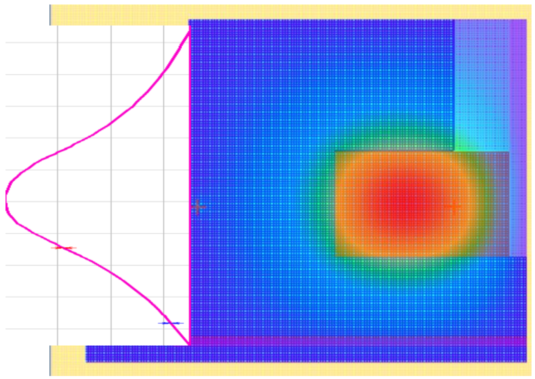

Magnetic field distribution

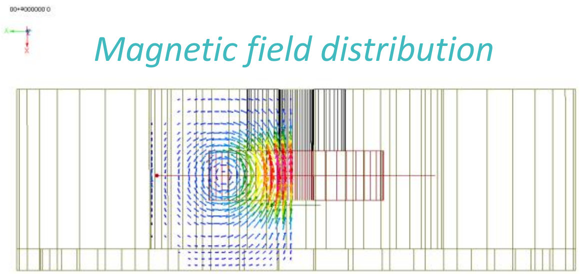

Electric field distribution

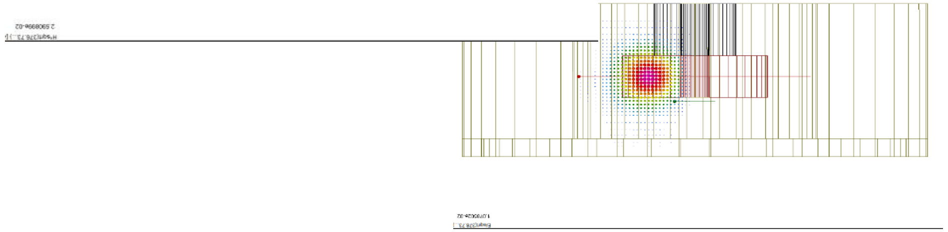

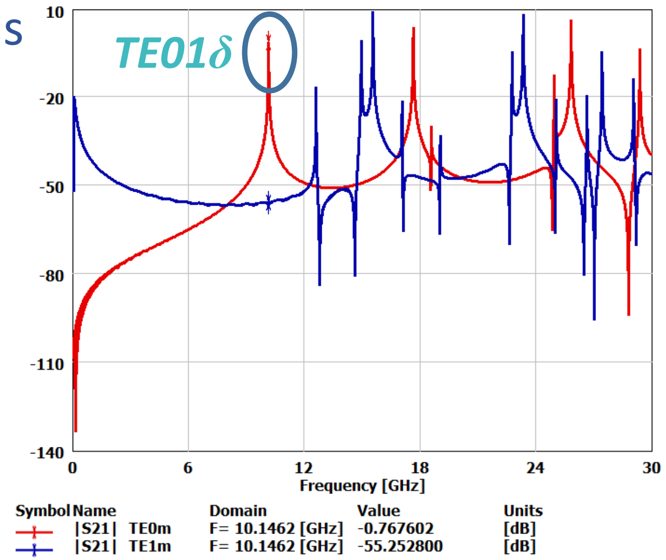

***TEnmδ* modes**
n=0
n=1

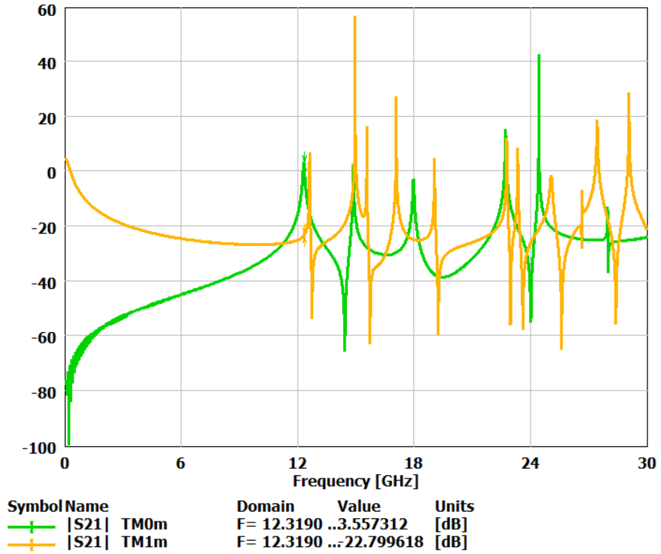

***TMnmδ* modes**
n=0
n=1

EM simulation results obtained with QuickWave software

2D imaging of material parameters – conducting materials (2)

Motorised 2D surface scanner

VNA
**courtesy Keysight Technologies, Austria*

Scanner Unit Control App

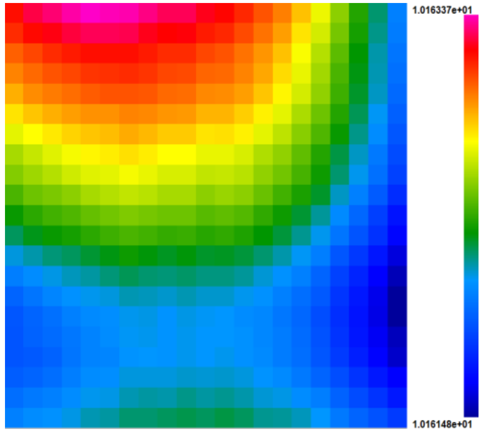

2D map of resonant frequency (in GHz) of 2D SiPDR scanner

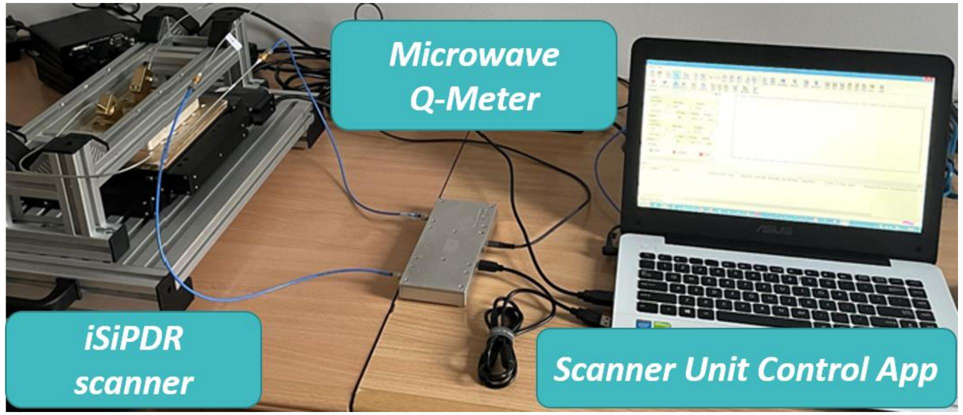

Graphene –based battery anode

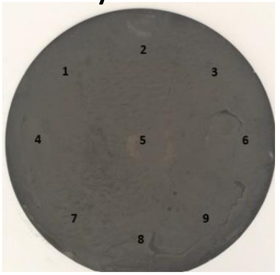

**courtesy PLEIONE Energy, Greece*

Semiconductor sample and its 2D resistivity map

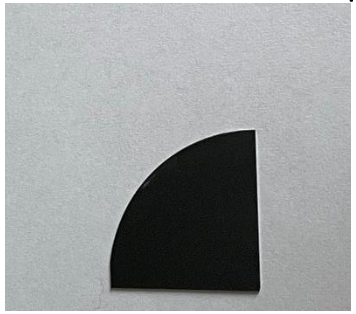

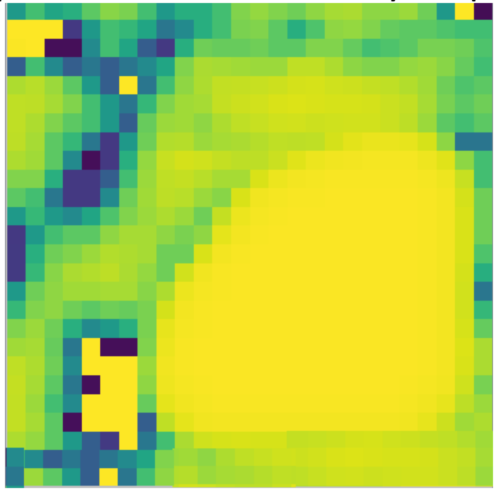

Dedicated measurement control software

SPDR & SiPDR measurement control app

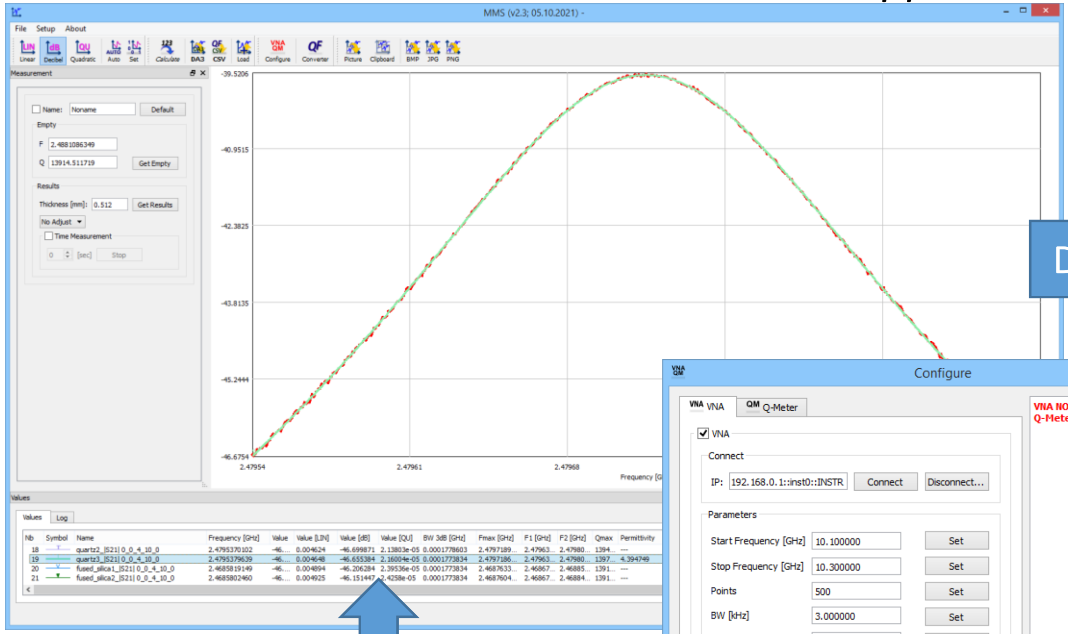

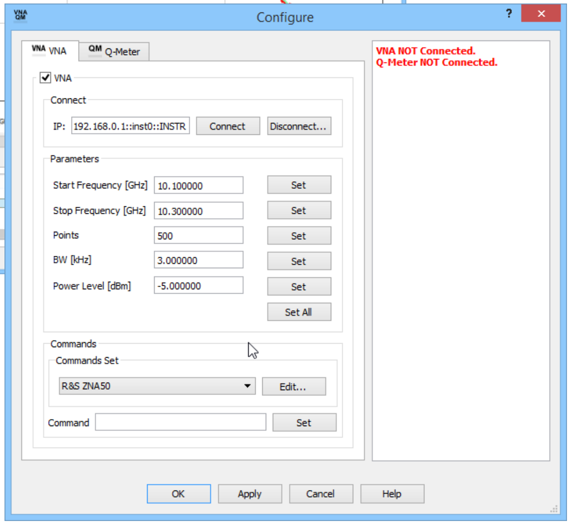

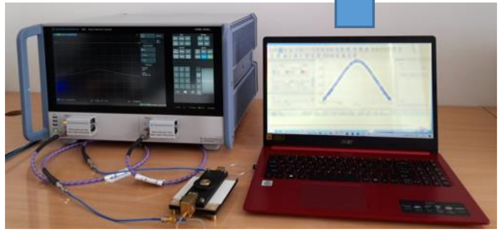

Development

Scanner Unit Control app

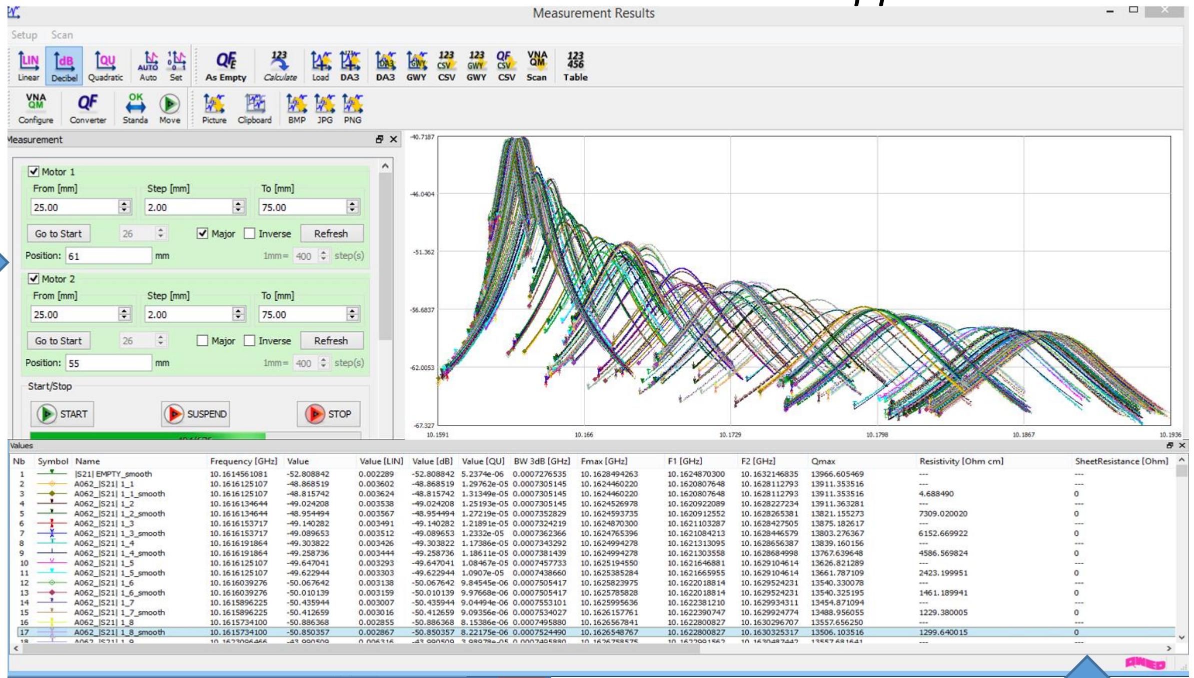

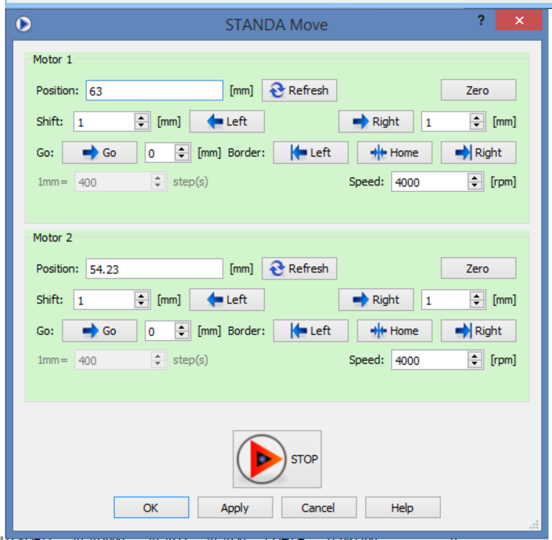

- ✓ Fully automated measurement procedure
- ✓ VNA/Q-Meter configuration, communication & control
- ✓ Built-in procedure for enhanced accuracy of Q-factor extraction
- ✓ Material parameters extraction
- ✓ Visualisation of measured material parameters values
- ✓ Import/export options

- ✓ Configuration and control of the motors and XY- translation table
- ✓ Export of scan results to *.csv and industrial *.gwy formats

Millimetre-wave characterisation of dielectric materials

Fabry-Perot Open resonator

Bridging the gap between classical resonant methods and free space methods

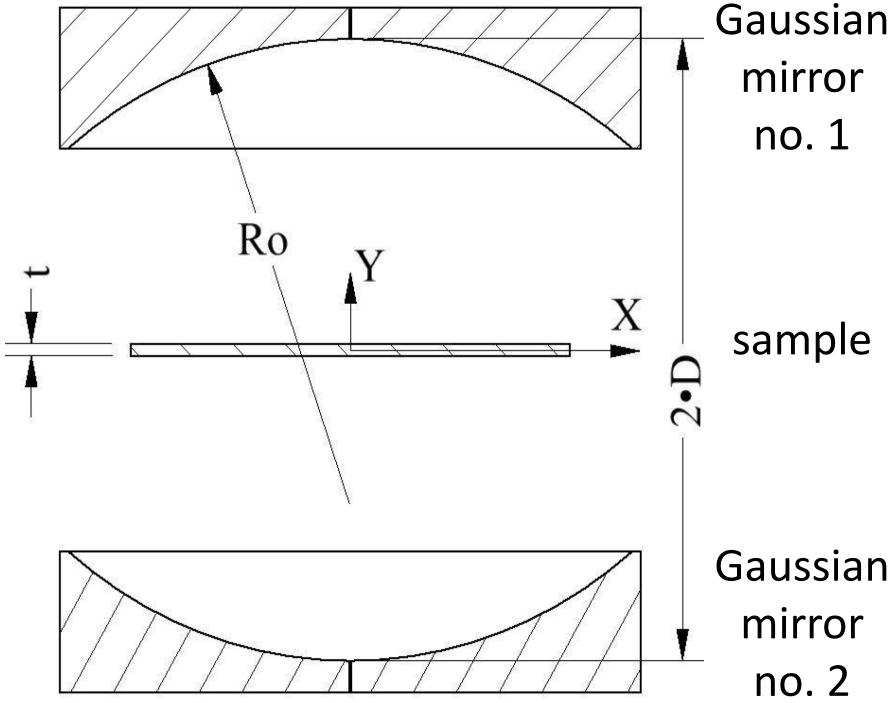

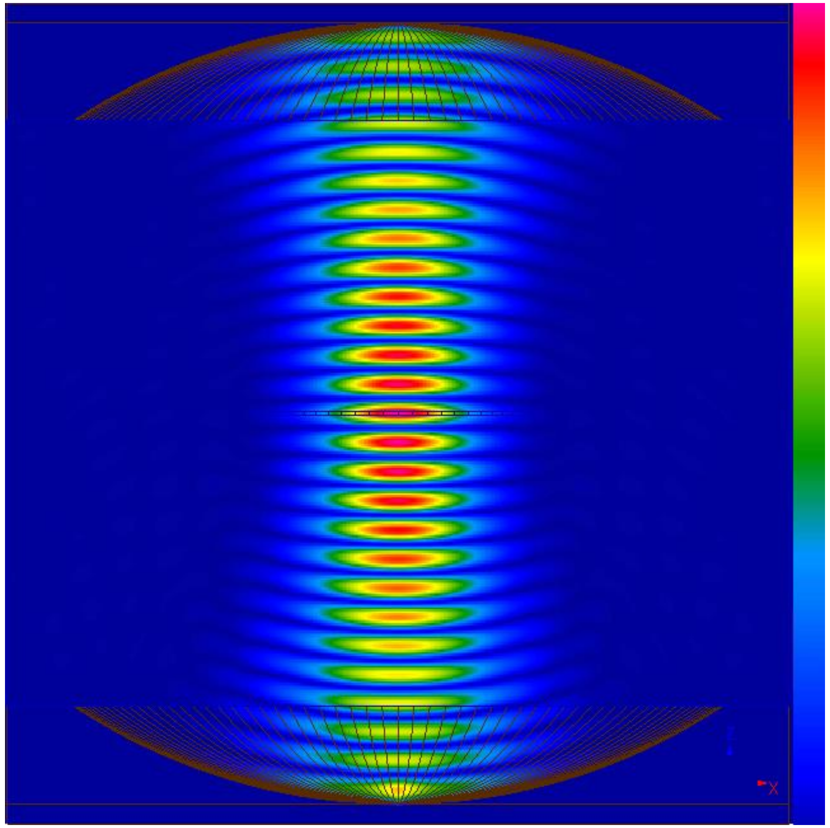

Electric field distribution - simulation model in QuickWave software

- Single device
- Spectrum: 20-110 GHz
- Frequency resolution: ca. 1.5 GHz
- Dk accuracy: $\Delta\varepsilon/\varepsilon < 0.5$ %
- Df range: $10^{-5} < \tan\delta < 10^{-2}$
- Sample diameter: > 3 inches
- Sample thickness: < 2 mm
- Fully automated measurement: (ca. 10 minutes in 20-50GHz)

Fabry-Perot Open Resonator (FPOR) – basics..

..and modeling

- the extraction of complex permittivity of a dielectric MUT is made with the aid of electromagnetic model
- classical solution is based on a characteristic equation
- novel EM model of the FPOR based on conformal transformation is employed
- reducing the FPOR's model to a scalar one-dimensional multilayer problem

→ *better accuracy than alternative solutions*

*Gaussian **TEM00q** modes*

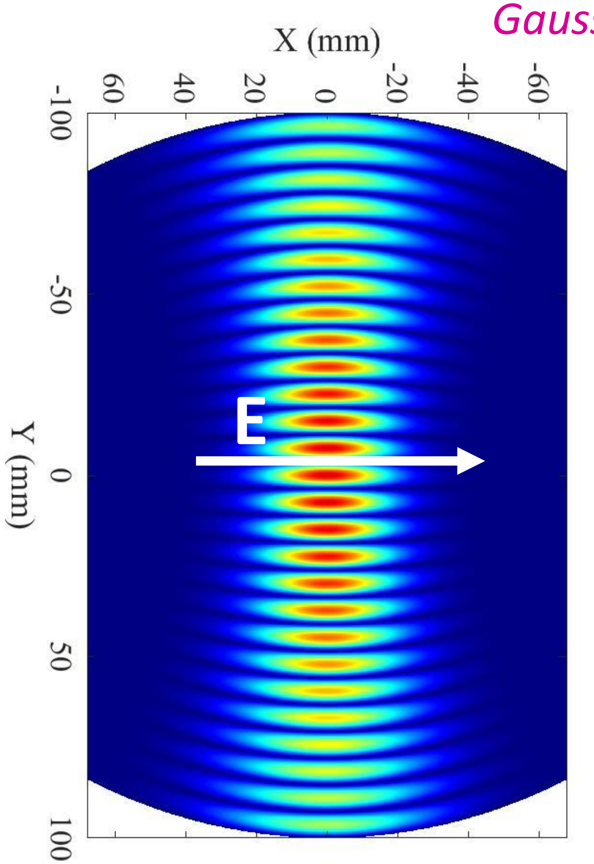

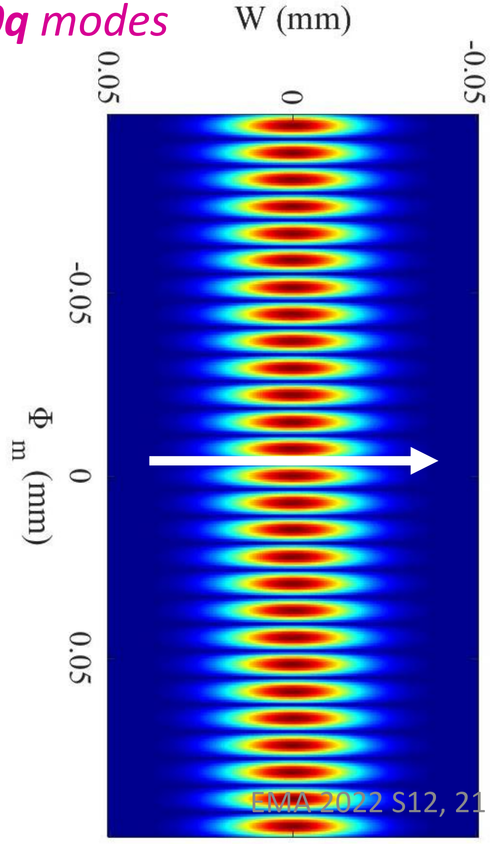

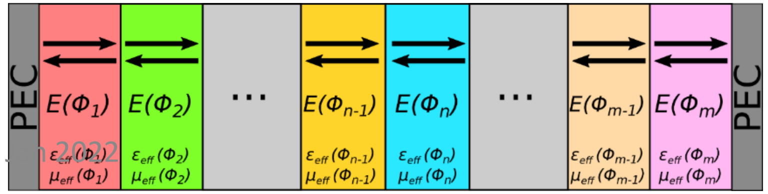

Fabry-Perot Open Resonator (FPOR) – measurement concept

Measurement:

Resonant frequency and Q factor

Electromagnetic model

simulation

Dielectric constant and loss tangent

@ multiple frequencies

Challenges for user

- mode identification
- mode tracking among plenty of other modes occurring in the FPOR

Solution

- Dedicated control software
- Automatic adaptive mode tracking algorithm
- No user intervention needed

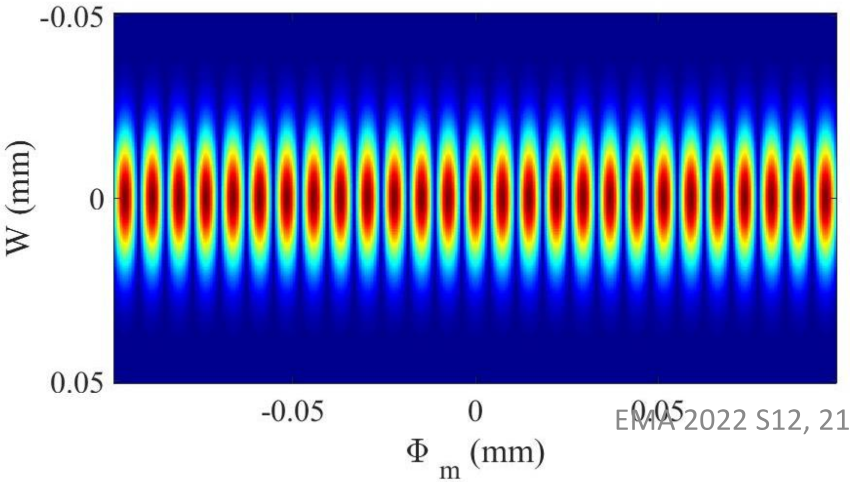

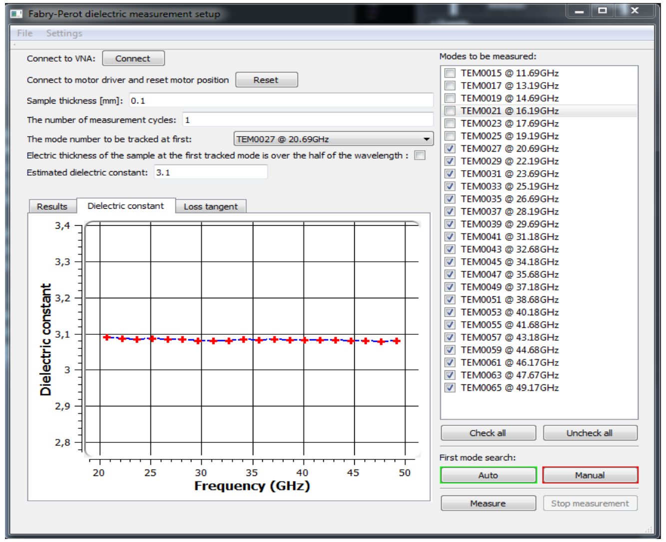

Fabry-Perot Open Resonator (FPOR) – results

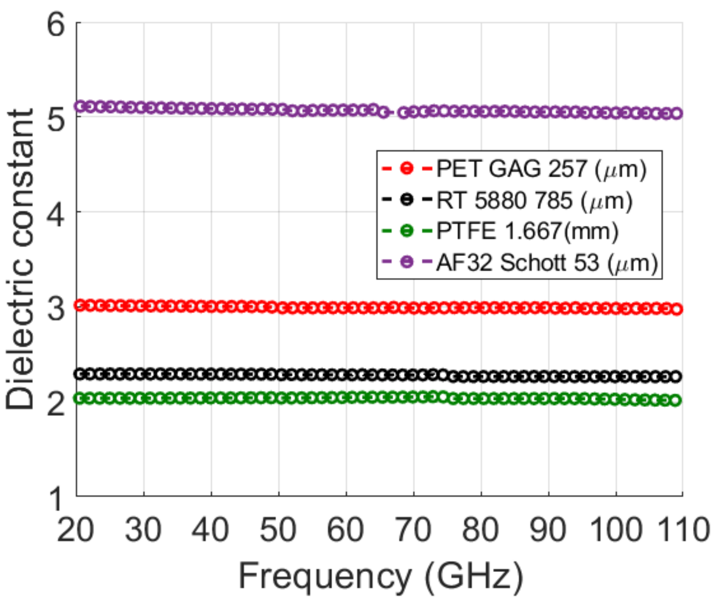

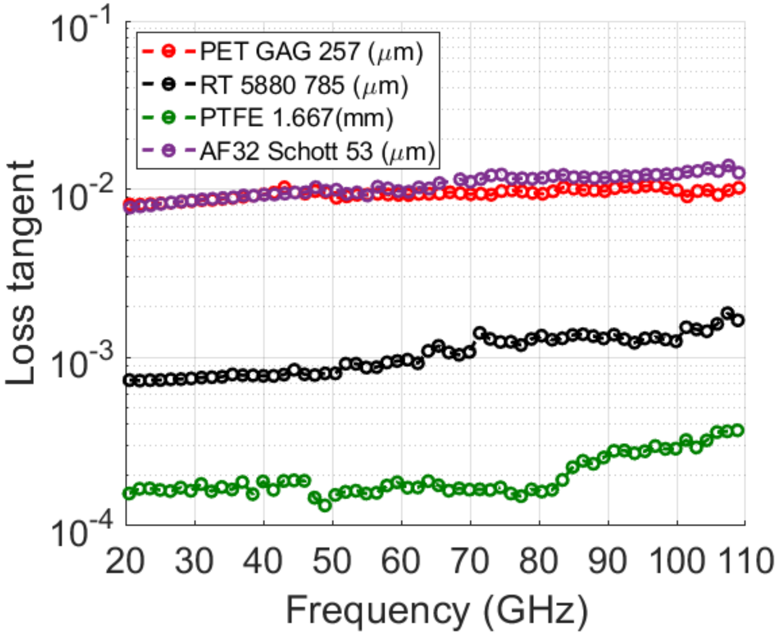

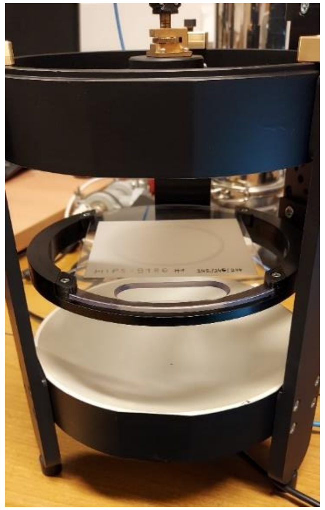

FPOR with a polystyrene (HIPS) sample placed on a sample holder

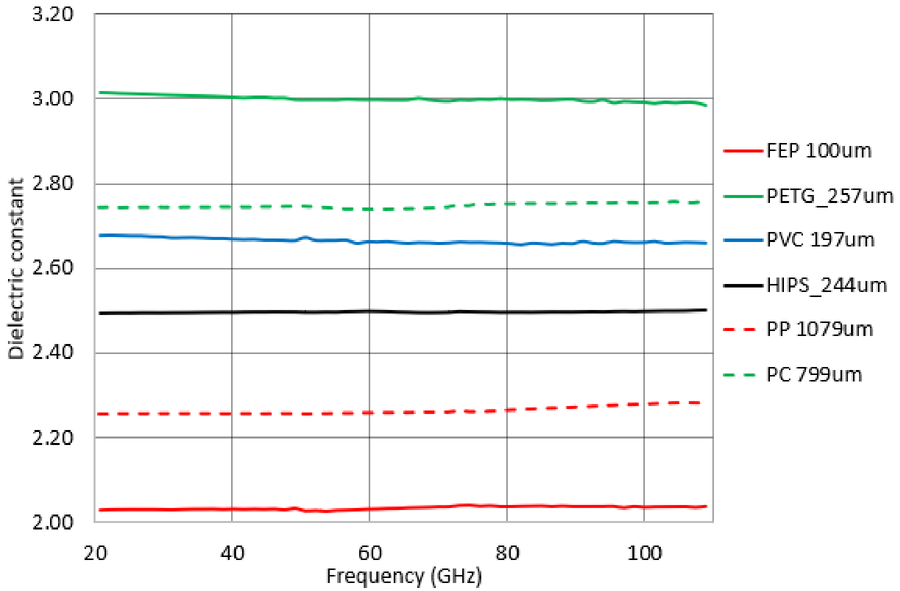

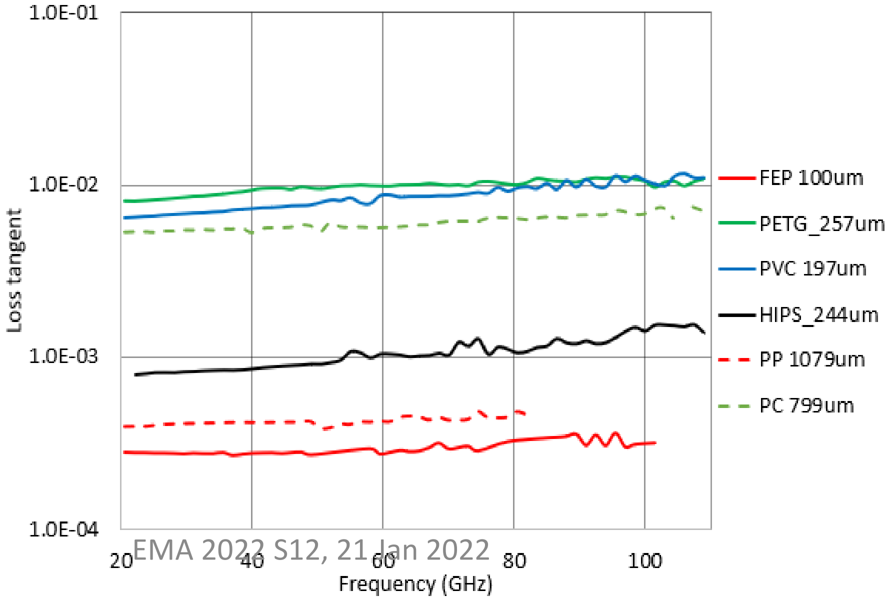

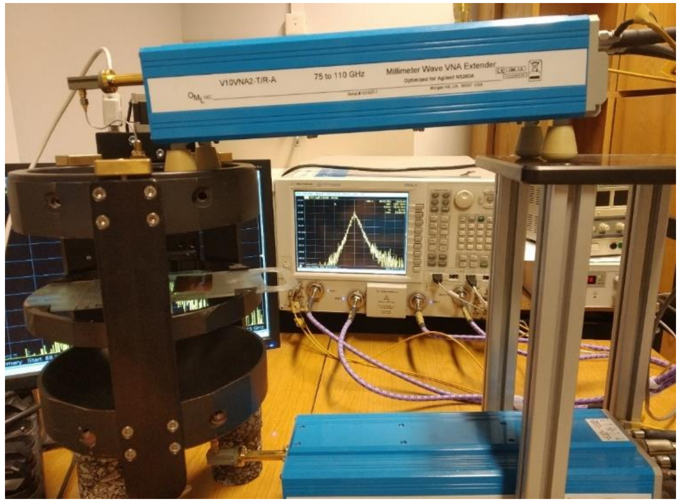

FPOR with OML frequency extenders operating in 75-110 GHz range.

Fabry-Perot Open Resonator (FPOR) – in-plane anisotropy

With appropriately designed feeding loops, FPOR is capable of linear E-field polarization and hence detecting in-plane anisotropy:

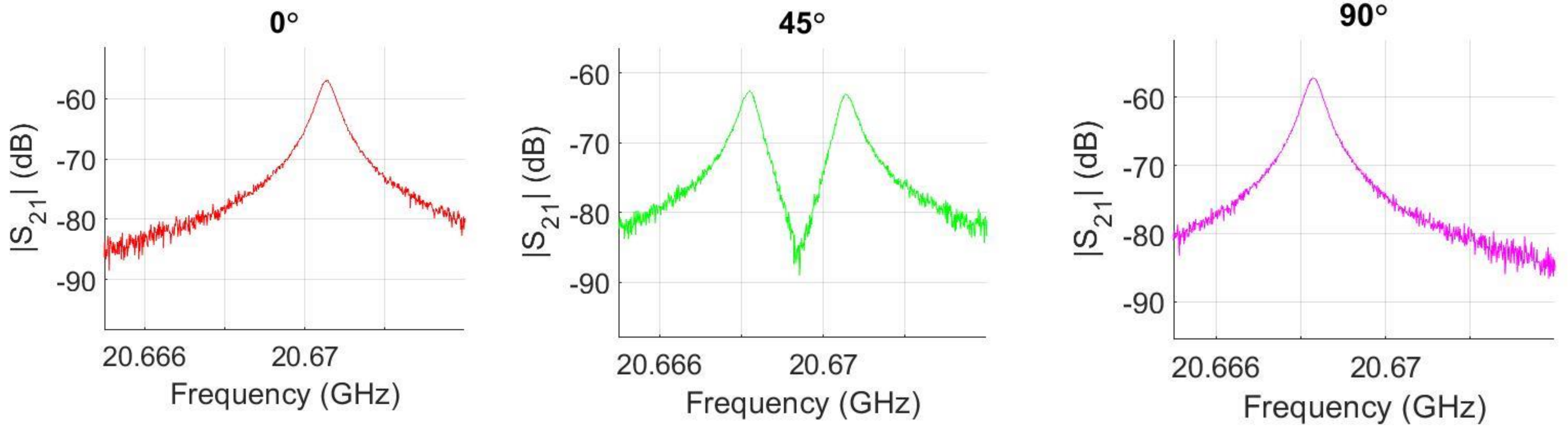

Resonances detected for BoPET sample (t = 0.100 mm), turned in xy plane.

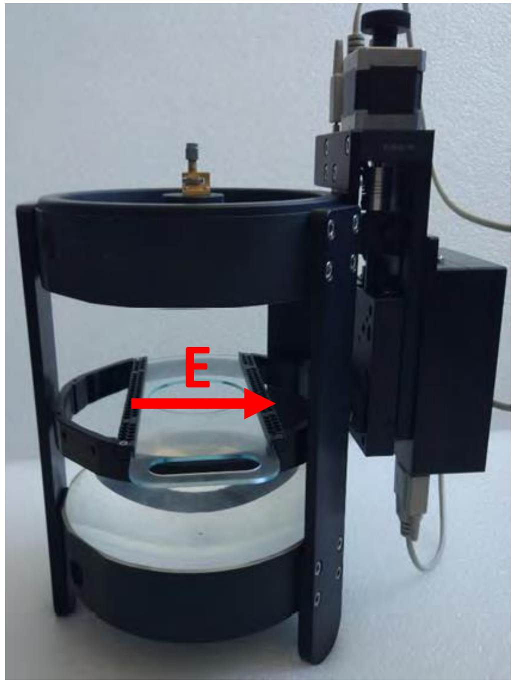

BoPET (biaxially-oriented PET) involves thermal drawing in two in-plane directions with substantially different draw ratios, followed by crystallization. Hence, it is in-plane anisotropic.

For PETG (non-crystalline copolyesters, isotropic), resonant frequency does not depend on angular position of the sample.

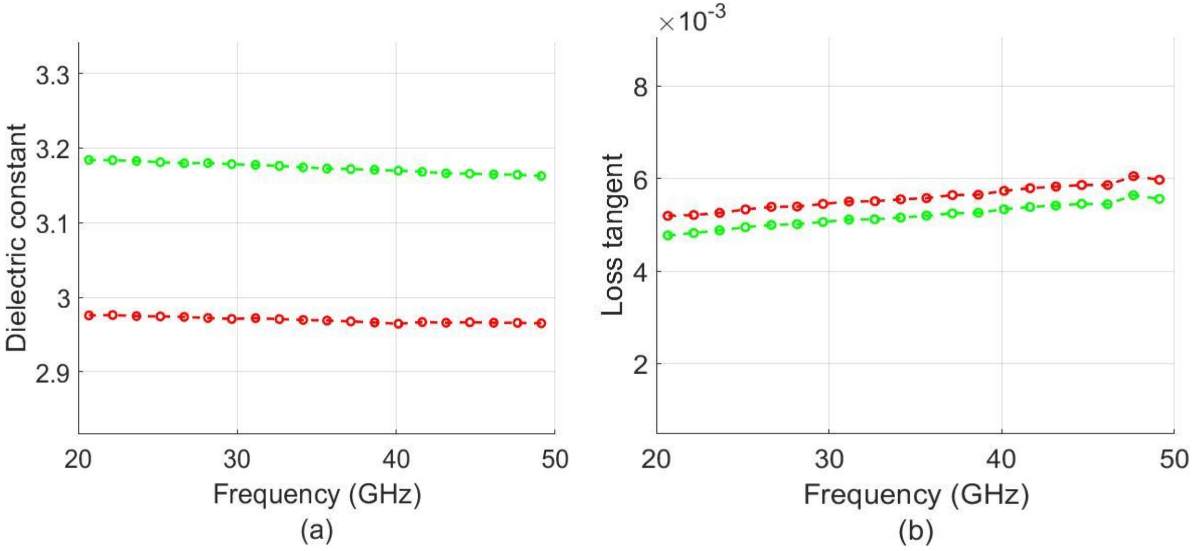

T.Karpisz et al, " Measurement of in-plane anisotropy of dielectric materials with a Fabry-Perot open resonator", Proc. MIKON 2020

On-going and future application to 5G materials

iNEMI

5G/mmWave Materials Assessment and Characterization

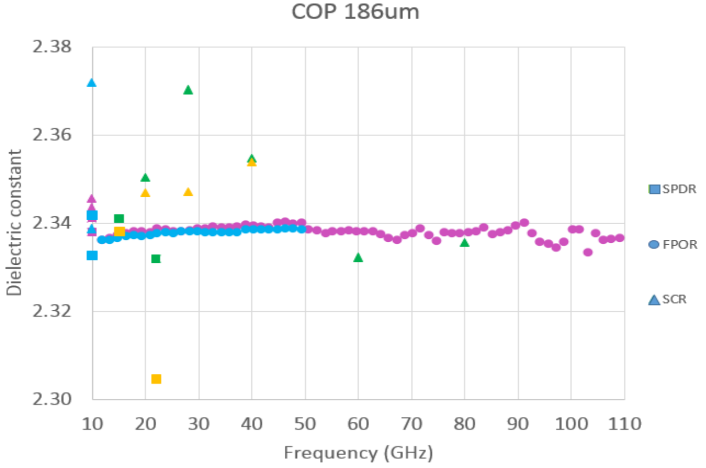

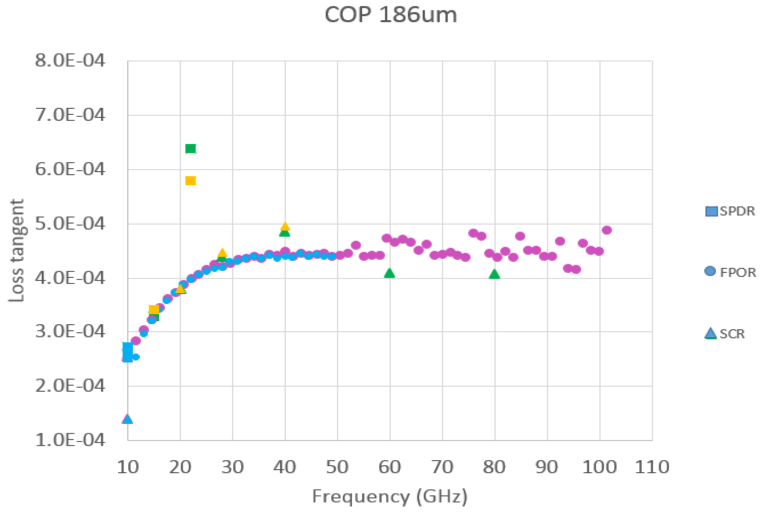

**M. Celuch et al., "Bridging the materials' permittivity traceability gap for 5G applications", IEEE Antennas & Propagation Symposium, 2021.*

Ultra-Low Temperature Co-fired Ceramics for 6th Generation Electronic Packaging

ULTCC6G_EPac« M-ERA-NET Joint Project Ref CEA : X40955

M-ERA.NET Fraunhofer IKTS

leti ceatech TECHNOLOGY RESEARCH INSTITUTE inoveos HYPERFREQUENCES EN PUISSANCE QWED Łukasiewicz IMiF

Measurements of multilayer ULTCC substrates with SPDR and FPOR techniques

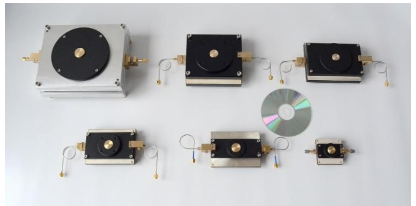

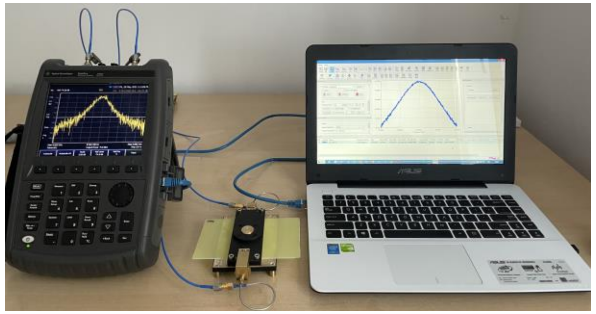

Measurements of bulk ULTCC composites

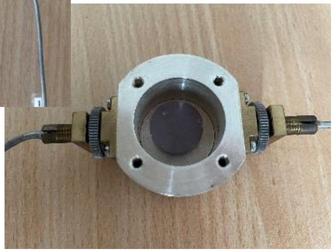

TE01delta cavity with a sample

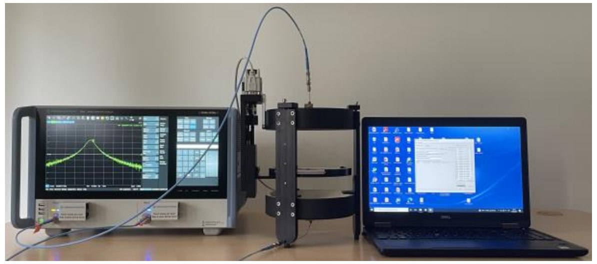

M-ERA-NET ULTCC6G_EPac project is co-financed by The National Centre for Research and Development under M-ERA.NET2/2020/1/2021 contract.

NCBR Narodowe Centrum Badań i Rozwoju

Acknowledgements

The work presented has received funding from the

European Union's Horizon 2020

research and innovation programme

under grant agreement

NanoBat No 861962.

(website: www.nanobat.eu)

Simulations conducted with QuickWave EM software, developed & commercialised by QWED.

The original designs of QWED resonators for material measurements from Prof. Jerzy Krupka, e.g.:

J. Krupka, A. P. Gregory, O. C. Rochard, R. N. Clarke, B. Riddle, and J. Baker-Jarvis, "Uncertainty of complex permittivity measurements by split-post dielectric resonator technique", *J. Eur. Ceramic Soc.*, vol. 21, pp. 2673-2676, 2001.

J. Krupka and J. Mazierska, "Contactless measurements of resistivity of semiconductor wafers employing single-post and split-post dielectric-resonator techniques," *IEEE Trans. Instr. Meas*., vol. 56, no. 5, pp. 1839-1844, Oct. 2007.

Conclusions

With this talk we seek collaborations:

on the development of:

- **material measurement test-fixtures,**
- **applicators for processing of materials,**
- **software models & workflows**

for 5G materials & applications.

on behalf of:

- **QWED team,**
- **our European projects NanoBat, ULTCC6G_EPac**
- **members of broader EU initiatives, e.g.**

European Materials Modelling Council.

THANK YOU!